Reviewer # 1 Questions and our responses

We thank Reviewer #1 for constructive comments and suggestions to improve our paper. In this section, we first list reviewer's questions/comments, and then provide our answers. The questions/comments are in italics, and our responses are in bold text.

In this paper, the authors proposed an unsteady analytical model for salt intrusion to understand the spatial-temporal dynamics of salt transport under different riverine and tidal forcing. The model was applied to the Humen estuary, which is a tide-dominated and well-mixed estuary. And the modelled results correspond well with the observed data. The paper is interesting and of important scientific implications for estuarine dynamics. However, there are still some major concerns that should be properly addressed before the paper can be accepted in this journal. Thus, I would suggest the authors to have a substantial revision.

Major concerns:

1. Method in Section 2: It is noted that a rather similar approach for salinity intrusion in an unsteady state was proposed by Song et al. (2008) entitled "One-dimensional unsteady analytical solution of salinity intrusion in estuaries". It is better to clarify the main difference between the current model and the one proposed by Song et al. (2008) in order to highlight the new insights into the salt dynamics.

The unsteady analytical model developed by Song et al. (2008) can reproduce the salinity process in an idealized estuary with constant depth and constant width. Song's model is thus applicable to laboratory flumes and artificial channels. However, the channel cross-sectional area of estuaries is typically converging. One innovation of our paper is to better capture the natural topography of alluvial estuaries, assuming the cross-sectional area to obey an exponential function. So, our paper continues on Song's work within the geometrical setting of an alluvial estuary. We will clarify this in the revision.

Song, Z. Y., Huang, X. J., Zhang, H. G., Chen, X. Q., and Kong, J.: One–dimensional unsteady analytical solution of salinity intrusion in estuaries, China Ocean Eng., 22, 113–122, 2008.

2. P8, Lines 19-24, estimation of the tidal excursion: Note that the tidal excursion is a critical parameter that links the salinity intrusion to the tidal hydrodynamics. In this study, the authors assumed that the longitudinal tidal excursion can be described an exponential function. However, such an assumption is only reasonable for a short channel (Let's say less than 10 km). I would suggest the authors to adopt an analytical hydrodynamics model to reproduce the longitudinal tidal excursion since there exists a long traditional analytical solution for tidal hydrodynamics in estuaries (e.g., Toffolon and Savenije, 2011; Winterwerp and Wang, 2013; Cai et al., 2016). The advantage of coupling the salinity intrusion model to the tidal dynamics lies in that it enables directly linking the salt dynamics into the tidal forcing (e.g., tidal amplitude imposed at the estuary mouth). Moreover, it allows to have a prediction of salinity intrusion for

different tidal forcing conditions (e.g., neap-spring changes) for given tidal amplitude observed at the estuary mouth. The current model used the observed salinity to forecast the tidal excursion (i.e., Eq. 18 in the manuscript), which is not very practical if prediction is required.

We appreciate the reviewer's suggestion and will use an analytical model for tidal hydrodynamics to compute the excursion length in the revised version. In the Method section, we will introduce Cai's method (Cai et al., 2016) as below:

"…We note that in the approach presented above the tidal excursion at the mouth is inferred from salinity data, whereas an alternative theoretical approach may be applicable that is less dependent on in situ data. Tidal wave propagation can be described analytically by a set of four implicit equations (Cai et al., 2012), the phase lag equation $\tan(\varepsilon)=\lambda/(\gamma-\delta)$**, the scaling equation** $\mu=\sin(\varepsilon)/\lambda$**, the damping equation** $\delta=\gamma/2-4\chi\mu/(9\pi\lambda)-\chi\mu^2/3$**, and the celerity equation** $\lambda^2=1-\delta(\lambda-\delta)$**, where λ is the celerity number** $\lambda=c_0/c$**, μ is the velocity number** $\mu=\upsilon\bar{h}/(r_s\eta c_0)$**, δ is the damping number** $\delta=c_0 \mathrm{d}\eta/(\eta \mathrm{d}x\omega)$**, and ε is the phase lag between HW and HWS** $\varepsilon=\pi/2-(\phi_Z-\phi_U)$ **. Here, three dimensionless parameters control the tidal hydrodynamics (Savenije et al., 2008), i.e. the dimensionless tidal amplitude** $\zeta=\eta/\bar{h}$**, the estuary shape number** $\gamma=c_0/(\omega a)$ **and the friction number** $\chi=r_s g c_0 \zeta/\left(K_s^2\omega\bar{h}^{4/3}\right)\left[1-(4\zeta/3)^2\right]^{-1}$**, where η is the tidal amplitude, K_S is the Manning-Strickler friction coefficient, r_s the storage width ratio, $\bar{h}$ is the tide-averaged depth and c_0 is the classical wave celerity** $c_0=\sqrt{g\bar{h}/r_s}$**. Then with available geometry and friction data at the estuary mouth, the tidal propagation celerity and the tidal amplitude (or the tidal excursion) can be obtained by solving the set of four equations…"**

In addition, we will apply the hydrodynamics model proposed by Cai et al. (2016) to the Humen estuary based on observations. The averaged depth along the axis of the Humen estuary is shown in Figure S1. The coefficient of determination R^2 is 0.67, which indicates that the topography is too complex to be represented by an exponential function. The water depth is influenced greatly by human activities. The input parameters used for the tidal hydrodynamics model will be summarized in Table S1. A new Figure S2a shows the computed tidal amplitude and the tidal excursion obtained with a hybrid model, using a variable depth along the estuary (Cai et al., 2012). The tidal amplitude along the Humen estuary can be well simulated by the analytical model while the tidal excursion is underestimated. There are two reasons which may cause the underestimation. The first one is due to the inaccurate estimation of the averaged depth along the estuary, since the depth convergence length *d* cannot be fitted well to the exponential function $\bar{h}=\bar{h}_0\exp(x/-d)$ **in the Humen estuary. It can have a serious impact on the three dimensionless parameters which control the tidal hydrodynamics, i.e. the dimensionless tidal amplitude, the estuary shape number and the friction number. The other one is the assumption that the tidal excursion is independent of the distance along the Humen estuary. Well, as was shown by Savenije (2005), the tidal excursion can be assumed to be constant in many estuaries worldwide. However,**

a conclusion from the measurement data show that the tidal excursion may be damped along the estuary, like in the Mekong Estuary. In four estuary branches, over more than 100 kilometers, tidal excursion decay can be described by an exponential function (Nguyen, 2008). In Figure S3a we will present the computed salinity curves using the calibrated variable tidal excursion along the Humen estuary. It better reproduces the salinity at HWS and LWS compared with the results obtained based on a hybrid model shown in Figure S3b. Therefore, similarly, the observations in the Humen estuary indicate that the tidal excursion decreases exponentially.

We agree with the reviewer that it is important to link the salinity intrusion to the tidal hydrodynamics. It can help the model to become applicable to a wider range of flow conditions. Therefore, the analytical hydrodynamics model by Cai et al. (2012) will be presented in the revised methods section. We will offer an analytical approach to reproduce the main tidal dynamics coupling to the salt dynamics. However, unfortunately, the analytical model for tidal dynamics cannot be used in this case, due to the limitations of available geometry as well as the assumption of the tidal excursion. So, in Section 4, we will provide another way to calibrate the tidal excursion based on the measurements of salinity.

Cai, H., Savenije, H. H. G., and Toffolon, M.: A new analytical framework for assessing the effect of sea-level rise and dredging on tidal damping in estuaries, J. Geophys. Res., 117, C09023, doi:10.1029/2012JC008000, 2012.

Cai, H., Toffolon, M., and Savenije, H.H.G.: An analytical approach to determining resonance in semi-closed convergent tidal channels, Coast Eng. J., 58(03), 1650009, 2016.

Nguyen, A. D.: Salt Intrusion, Tides and Mixing in Multi-Channel Estuaries: PhD: UNESCO-IHE Institute, Delft. CRC Press, 2008, p52.

Savenije, H. H. G.: Salinity and Tides in Alluvial Estuaries, Elsevier, Amsterdam, 2005.

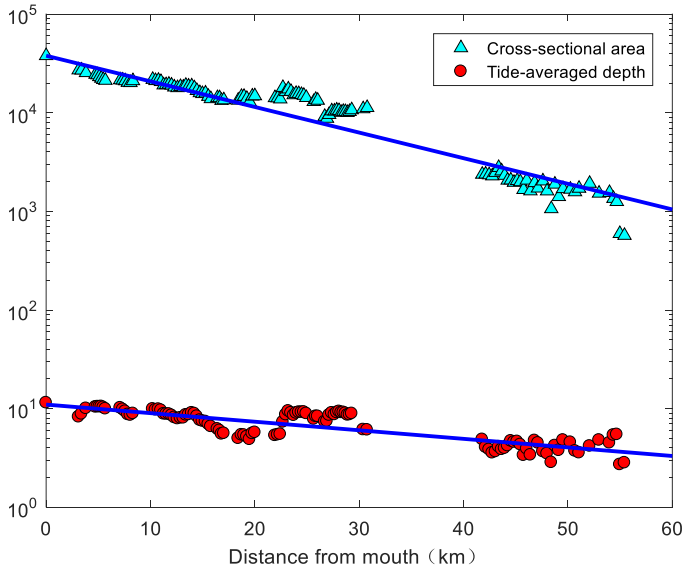

Figure S1: Shape of the Humen estuary, showing the correlation between the cross-sectional area A (m^2) and averaged depth $\bar{h}$ along the estuary axis with fitted trend lines.

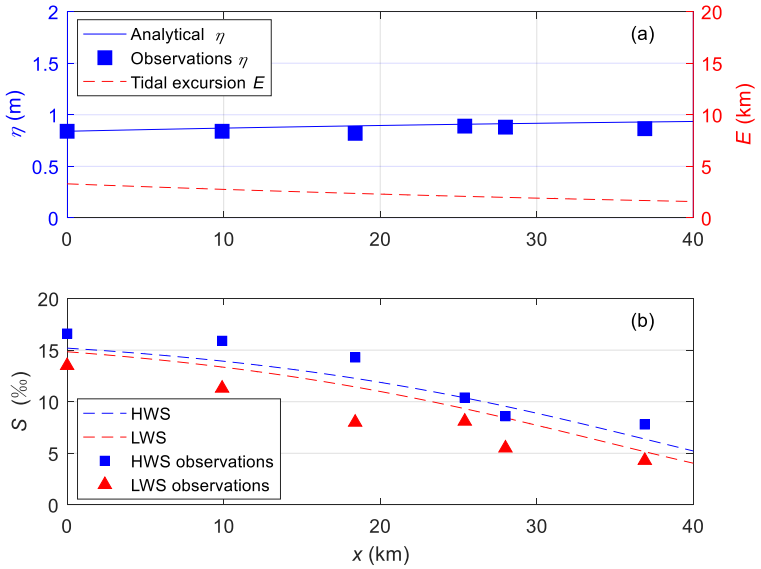

Figure S2: (a) The computed tidal amplitude and tidal excursion in the Humen estuary based on a hybrid model using a variable depth along the estuary; (b) Comparison between computed salinity and the observations at HWS and LWS. The tidal excursion is computed with a hybrid model.

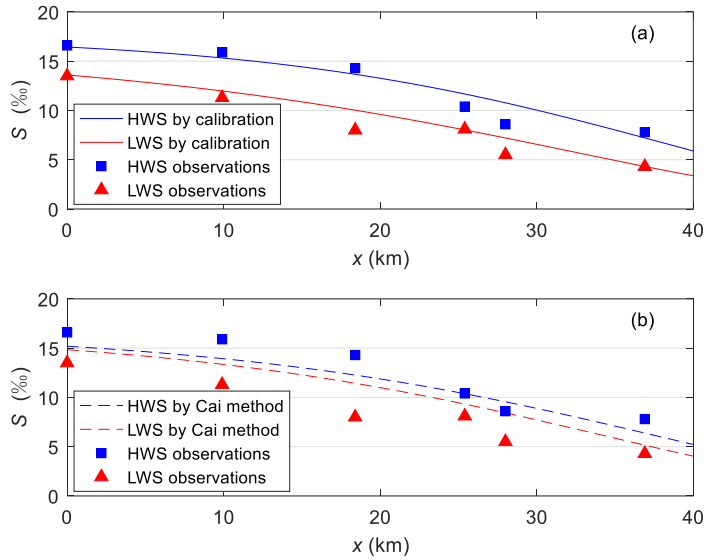

Figure S3: (a) Comparison between the observed and computed salinity curve using the calibrated tidal excursion; (b) Comparison between the observed and computed salinity curve based on a hybrid model using a variable depth along the estuary.

Table S1: Inputs used for the tidal hydrodynamics model

	A (m^2)	a (km)	h_0 (m)	d (km)	η_0 (m)	Ks ($m^{1/3}s^{-1}$)	T (s)	s_0 (‰)
Humen	**37822**	**16.7**	**10**	**50**	**0.84**	**35**	**44400**	**15.02**

3. P8, Lines 25-29, estimation of the wave celerity: Similar to the tidal excursion, I would suggest the authors to link the wave celerity to the tidal forcing imposed at the estuary mouth by means of an analytical model for tidal hydrodynamics.

The analytical hydrodynamics model (Cai et al., 2012) will be presented in the method section in the revised version, but it does not apply to our specific field case.

Cai, H., Savenije, H. H. G., and Toffolon, M.: A new analytical framework for assessing the effect of sea-level rise and dredging on tidal damping in estuaries, J. Geophys. Res., 117, C09023, doi:10.1029/2012JC008000, 2012.

4. For the time being, the authors only illustrate the proposed analytical model applied to the Humen estuary during the neap tide condition, when the salt intrusion length is approximately minimum. I would suggest the authors to adopt the model to the case during the spring tide condition when the salt intrusion really matters. In section 4.2 concerning the model validation, since the authors only used the dataset from Jan. 29th to Feb. 3rd, I think this is only kind of the model calibration rather than validation because the tidal hydrodynamics is more or less the same during the chosen period.

In the study, the salinity is assumed to be forced by a harmonic tidal wave with a single-frequency. So our model is more applicable for estuaries with semidiurnal tides or diurnal tides. It is found that the semidiurnal tide is the distinctively dominant tidal wave in the neap tide in Humen, while the diurnal tide is as important as the semidiurnal tide in the spring tide. Therefore, we chose the data during the neap tide to illustrate our unsteady model in this case.

We have rewritten Section 4 to make it clearer in the revised version. The calibrated parameters include tidal excursion *E* and dispersion coefficient *D*. Although each of the calibrated dispersion coefficients from 29 January to 3 February was listed in Table 2, in fact, only the one on 29 January was used for calibration. In other words, we use the data on 29 January to calibrate the parameters of the model and use the data from 30 January to 3 February to validate the model. To make it clearer, in the revised version, we use two figures to show the results, Figure 4 is the calibrated result and Figure 5 is the validation results, as below:

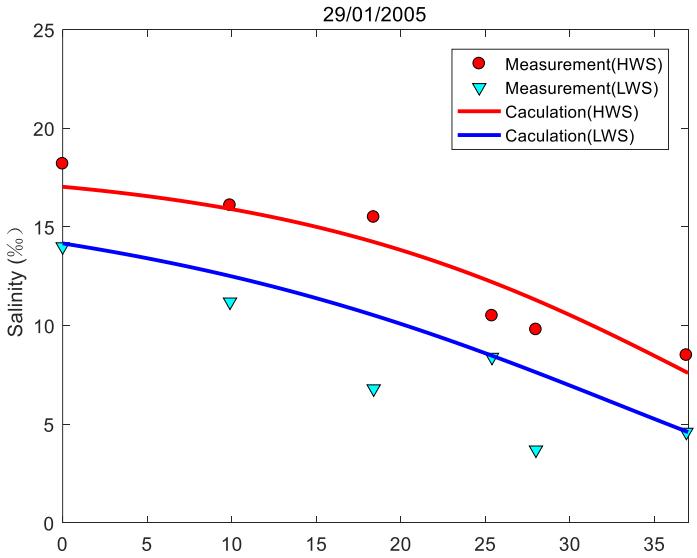

Figure 4: Comparison between calibration result and measured salinity concentration along the river on 29 January, 2005, showing values of measured salinity at high water slack (circle) and low water slack (inverted triangle), and the calibrated salinity curves at high water slack (red curve) and low water slack (blue curve).

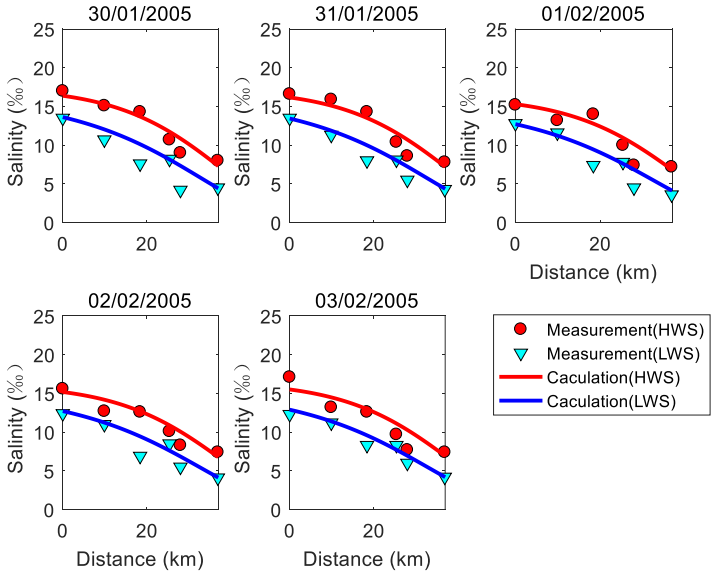

Figure 5: Comparison between validation result and measured salinity concentration along the river from 30 January to 3 February, 2005.

5. Sensitivity analysis: As mentioned by the authors, the proposed analytical model can directly reflect the influence of the tide and the interaction between the tide and runoff (see Abstract part in Line 17). Hence, it is better to conduct a sensitivity analysis of the salinity distribution to both the tidal and riverine forcing imposed at both ends of the estuary.

We appreciate the reviewer's suggestion and add a "Sensitivity analysis" part in the revised version, as below:

"The amplitude of salinity can be described by:

$$\hat{s} = \overline{s}_x * I_s \text{,} \quad \textbf{(23)}$$

where $\overline{s}_x$ is the tide-averaged salinity along the estuary and is a function of the river discharge, i.e. Eq.(12). The parameter I_s is the salinity amplitude coefficient that is defined as:

$$I_s = -\frac{EQ_f}{2DA} \text{,} \quad \textbf{(24)}$$

representing the interaction between tides and the river discharge. To investigate the longitudinal salinity distribution and intratidal salinity variation for different discharge and tidal dynamic conditions in the Humen estuary, Eqs. (12) and (23) are used to plot the longitudinal salinity curve and intratidal variation of salinity, respectively. The implemented parameters are the same as shown in Table 3, only the river discharge and the tidal excursion are variable.

Three constant discharge values of 200, 600 and 1800 m^3/s are used to evaluate the impact of the river discharge on the salinity variation. The discharge values are chosen because the minimum discharge in the dry season is around 600 m^3/s in the Humen estuary, and low salinity can be measured at Huangpuyou station when the discharge is larger than 1800 m^3/s. In addition, the discharge in the extreme dry season is set to be 200 m^3/s. The longitudinal salinity curve can be seen Figure 9a. At tidal average conditions, the salt intrusion length becomes smaller when the discharge increases. The steepest salinity gradient can be found at the highest discharge (Q_f=1800 m^3/s). It is clear from Figure 9b that the salinity amplitude increases firstly and then decreases as the river discharge increases. This is because during periods of low river discharge (Q_f= 200 m^3/s), the tide-averaged salinity is larger but the salinity amplitude coefficient I_s is smaller, which indicates the weaker interaction between the river flow and the tides. However, the tide-averaged salinity decreases rapidly with the increasing river discharge as we can see from Figure 9a, resulting in a smaller amplitude of salinity during periods of high river discharge (Q_f= 1800 m^3/s).

The tidal effect is studied using three different tidal excursions. The tidal excursion values result in the plots that is shown in Figure 10. The longitudinal salinity distribution at tidal average conditions is independent of the tidal excursion, as can be seen in Figure 10a. From Eq. (23), since the salinity amplitude coefficient I_s is in direct proportion to the tidal excursion, the amplitude of the salinity shows a linearly increasing trend with the increased tidal excursion (Figure 10b)."

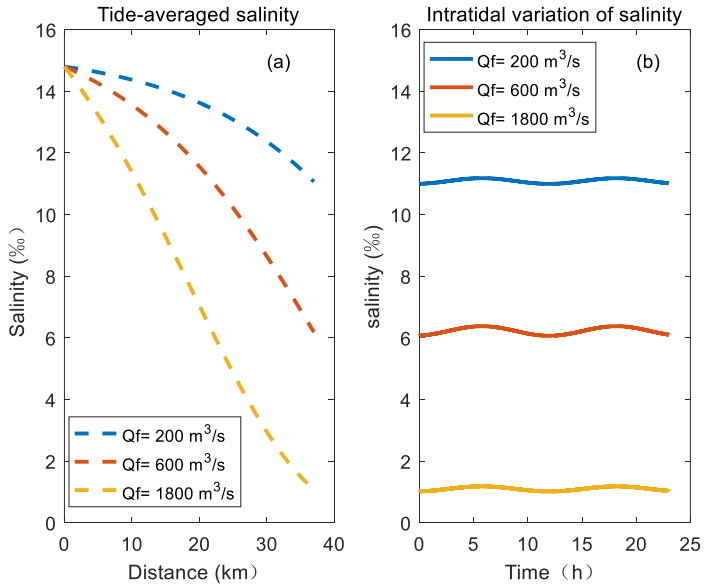

Figure 9: (a) Longitudinal salt intrusion curve at Tidal average considering different river discharge; (b) intratidal variation of salinity at Huangpuyou station on 31 January, 2005 considering different river discharge.

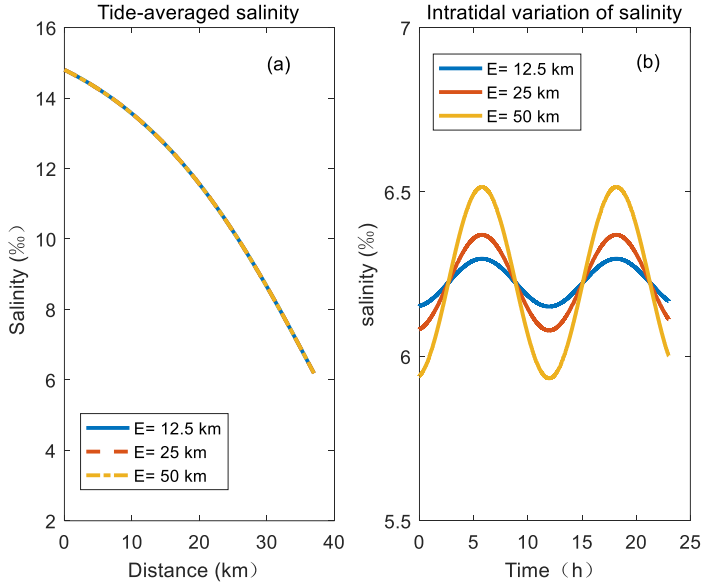

Figure 10: (a) Longitudinal salt intrusion curve at Tidal average considering different tidal excursion; (b) intratidal variation of salinity at Huangpuyou station on 31 January, 2005 considering different tidal excursion.

Minor concerns:

1. P3, Eq. (3) and Eq. (4): Here please clarify the physical meaning of s1 and s2 coefficients. In addition, it is noted that the salinity and velocity are assumed to be in phase since they have the same initial phase, am I right? Please also clarify this important assumption.

In fact, Eq. (3) is the expression of salinity using a first-order Fourier expansion method. Therefore, mathematically, s1 and s2 are the Fourier

expanding coefficients, and the physical meaning is the amplitude of salinity variation. Since the value of the initial phase in Eq. (3) has no impact on the Fourier expansion, we assume the salinity having the same initial phase with the velocity for convenience of calculating.

2. P7, Line 18: Please clarify where the salinity was sampled. It was sampled in the central part of the channel or near side banks? Due to the fact that the model used the cross-sectional averaged salinity concentration, it would be better to clarify this point.

Considering the impact of the shipping, the measuring positions were near the banks, with certain distances ranging from 605 m to 70 m.

3. P9, Lines 14-16: It is better to illustrate the stratification or mixing during the studied period since the authors already collected both the surface and bottom salinity concentration.

The field survey was carried out by Guangdong Province Hydrology Bureau and the Pearl Hydrology Bureau from the River Conservancy Commission. Unfortunately, they only provided us the vertically averaged salinity at each measuring location, related to the well-mixed condition in Humen estuary. For lack of the vertical salinity data, we further support this view in the revised version, as below:

"…The Humen estuary is well-mixed under normal flow conditions during the dry season (Ou, 2009; Luo et al., 2010). Due to three years of drought, the river discharge decreased by 50 percent during the study period in 2005 compared to a normal year (Liao, Pan, and Dong, 2008). Thus, there is no doubt that well-mixed conditions prevailed during the calibration and validation…"

Liao, D.Y.; Pan, T.J., and Dong, Y.L., 2008. Characteristics of salt intrusion and its impact analysis in Guangzhou. Environment, S1, 4-5. (In Chinese)

Luo, L., Chen, J., Yang, W., and Wang, D.X, 2010. An intensive saltwater intrusion in the pearl river delta during the winter of 2007–2008, J. Trop. Oceanogr., 6, 22-28. (In Chinese)

Ou, S.Y., 2009. Spatial difference about activity of saline water intrusion in the Pearl River Delta. Scientia Geographica Sinica, 29(1), 89-92. (In Chinese)

4. P11, Lines 6-8: Due to the assumptions of Eqs. (3)-(4), the extreme values of salinity appear when the tidal velocity is zero.

In physical terms, the tidal flow moves in the reversed direction just in the next tick when the tidal velocity turns into zero. At that moment, the salinity at the study site is the maximum or minimum value. Savenije (2005) also assumed that the maximum salinity is reached when tidal discharge is zero.

Savenije, H. H. G.: Salinity and Tides in Alluvial Estuaries, Elsevier, Amsterdam, 2005, p141.

5. Figure 1: Please use 'West River' and 'North River' instead of 'Xijiang River' and 'Beijiang River', respectively. Meanwhile, it is better to indicate the locations of outlets

that were mentioned in the main text.

We appreciate the reviewer's suggestion and redraw Figure 1 in the revised version as below:

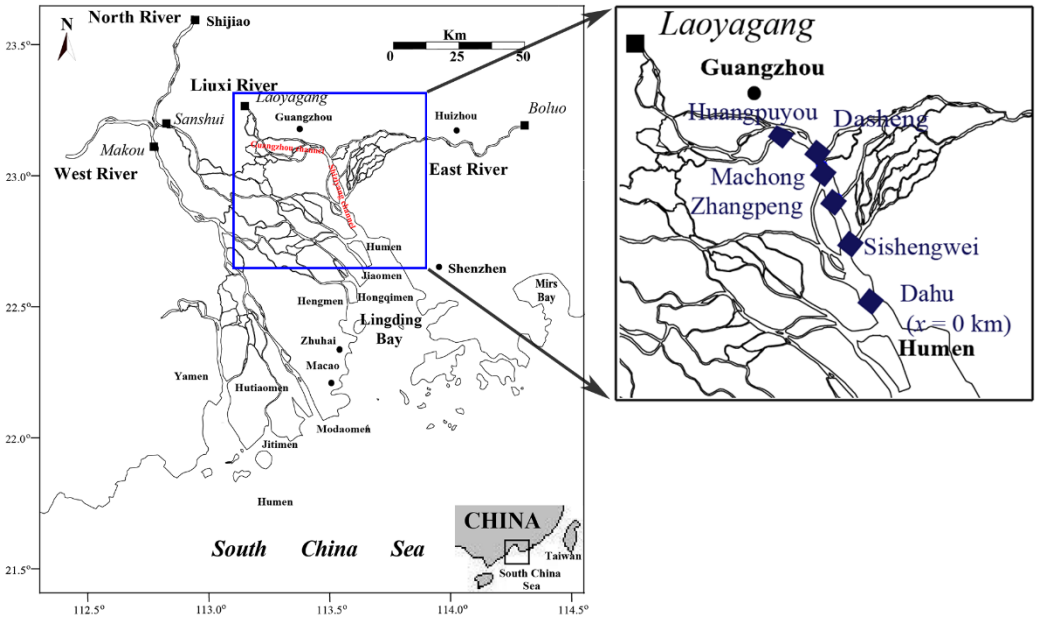

Figure 1: Map of the Humen estuary, showing the gauging stations where salinity concentration was measured during the field survey from 29 January to 3 February, 2005.

6. Figure 2: It is better to use the logarithm scale.

We will use a logarithmic scale in the revised version as below:

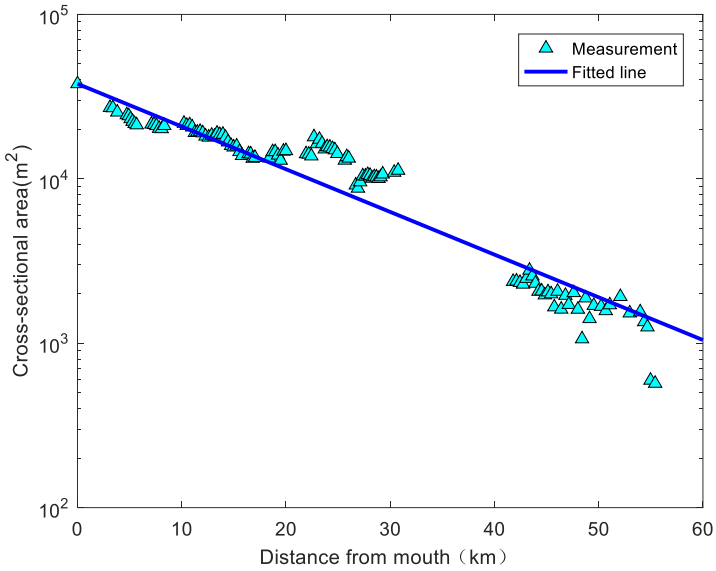

Figure 2: Shape of the Humen estuary, showing the correlation between the cross-sectional area A (m^2) and the distance from the estuary mouth x (km). The coefficient of determination R^2 is 0.92. The triangles represent observations and the line represents the fit to Eq. (1), where the area at the estuary mouth A_0=37822 m^2 and the area convergence length (a) is 16.7 km.

7. Figures 4, 6, 7: Please relocate the legend to a suitable place.

We appreciate the reviewer's suggestion and redraw Figures 4, 6 and 7 in the

revised version as below:

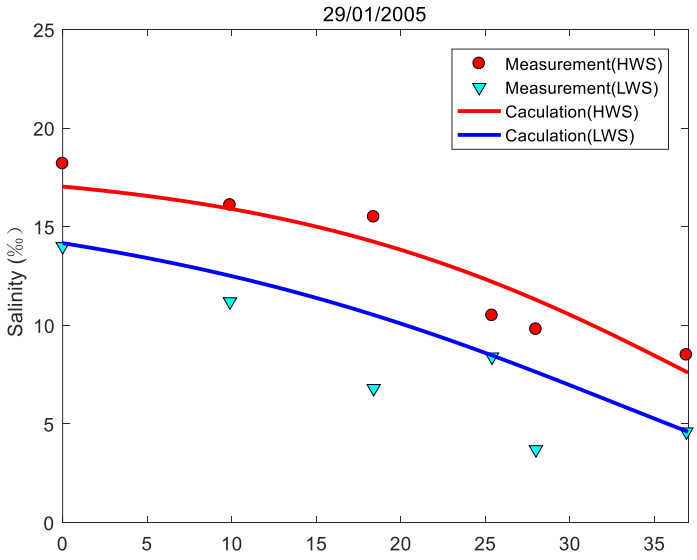

Figure 4: Comparison between calibration results and measured salinity concentration along the river on 29 January, 2005, showing values of measured salinity at high water slack (circles) and low water slack (inverted triangles), and the calibrated salinity curves at high water slack (red curve) and low water slack (blue curve).

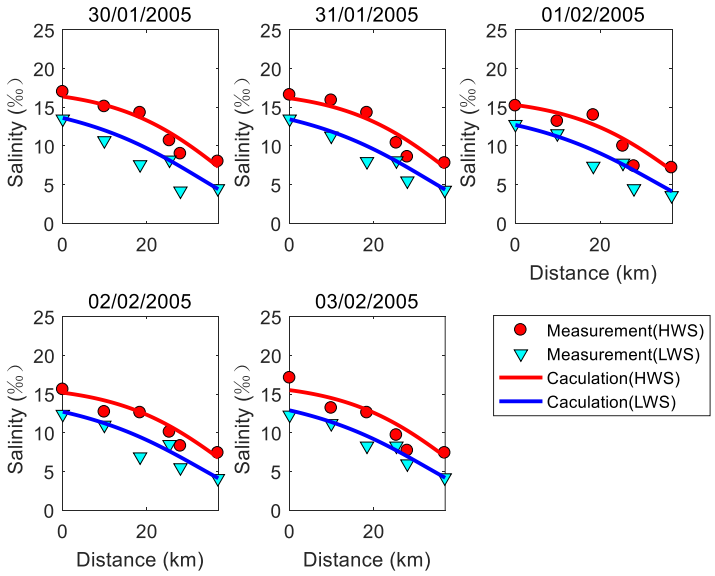

Figure 5: Comparison between validation result and measured salinity concentration along the river from 30 January to 3 February, 2005.

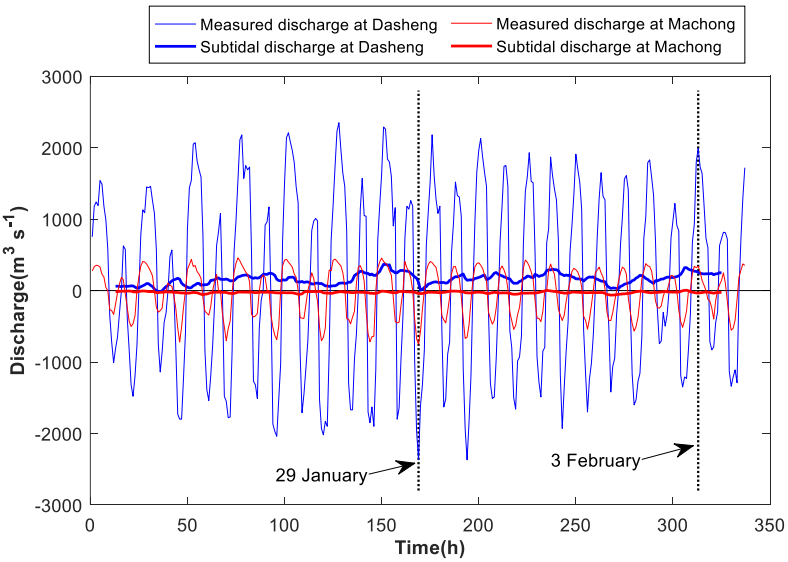

Figure 7: Subtidal discharge measured at Machong station and Dasheng station from 29 January through 3 February. Positive values mean seaward.

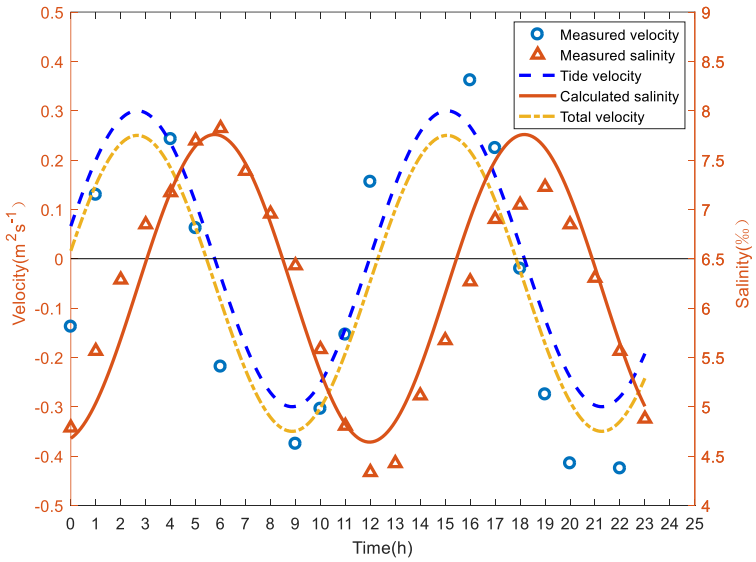

Figure 11: Salinity and tidal flow velocity over a tidal cycle at Huangpuyou station. The measured salinity is represented by triangles and the measured flow velocity is indicated by circles (on 31 January 2005). The dashes line is the calculated tidal velocity while the dash-dotted line is the total velocity of tidal flow and river flow. The red solid curve represents salinity simulated by the unsteady analytical solution, which reproduces the time lag HWS and maximum salinity.

References：

Cai, H., Toffolon, M., Savenije, H.H.G., 2016a. An analytical approach to determining resonance in semi-closed convergent tidal channels, Coast Eng. J., 58(03), 1650009.

Toffolon, M., Savenije, H.H.G., 2011. Revisiting linearized one-dimensional tidal propagation. J. Geophys Res., 116. DOI:ArtnC0700710.1029/2010jc006616

Winterwerp, J.C., Wang, Z.B., 2013. Man-induced regime shifts in small estuaries-I: theory. Ocean Dynam., 63(11-12): 1279-1292. DOI:10.1007/s10236-013-0662-9

Reviewer # 2 Questions and our responses

We thank Reviewer #2 for excellent comments and suggestions, which helped us to improve our paper. In this section, we first list the reviewer's question/comment, and then provide our answer. The questions/comments are in italics, and our response is in bold text.

In this manuscript, an unsteady analytical solution was presented to simulate the spatial-temporal variation of salinity in convergent estuaries and applied to the Humen estuary of the Pearl River Delta. There are a lot of issues which should be addressed.

Major points:

1. This manuscript is about the unsteady state analytical model for salt intrusion, but in the introduction section there is no anything about unsteady state analytical model. Nobody else did the unsteady state analytical model?

At present, there are few studies presenting unsteady state analytical models to analyze the intratidal variation of salinity. Song et al. (2008) have proposed one applicable to laboratory flumes and rectangular canals, in a Chinese journal. We refer to this study in the introduction of the revised version, as below:

"…Few studies have focused on analyzing the intratidal variation of salinity analytically. Song et al. (2008) proposed an unsteady-state model applicable to laboratory flumes and artificial channels where the cross section is assumed to be constant along the channel. Elaborating on the work of Song et al. (2008), here, an unsteady-state model is developed to predict the intratidal salinity intrusion dynamics in alluvial estuaries where the cross-section area typically converges..."

Song, Z. Y., Huang, X. J., Zhang, H. G., Chen, X. Q., and Kong, J.: One–dimensional unsteady analytical solution of salinity intrusion in estuaries, China Ocean Eng., 22, 113–122, 2008.

2. What differences are there between your model and previous models? What are the advantages of your model? Authors should compare your model results with other model results, to prove that your model is better.

The unsteady analytical model developed by Song et al. (2008) can reproduce the salinity process in an idealized estuary with constant depth and constant width. Therefore, Song's model is best applicable to laboratory flumes and artificial channels. However, the convergence of cross-sectional area of estuarine channels is crucial. One innovation of this paper is to make use of the natural topography of alluvial estuaries, where the cross-sectional area development along the channel obeys an exponential function. So, our paper continues on Song's work within the geometrical setting of an alluvial estuary.

3. In the methods section, which are input parameters, and how to determine them? These should be presented clearly.

The input parameters include the tide-averaged salinity at the mouth, the convergence length of cross section *a*, the dispersion coefficient *D*, the tidal

excursion E_0, the damping length of the tidal excursion e, the initial phase φ_0 and the tidal celerity c. We provide two approaches to estimate the calibrated input parameters. In the method section of the revision, we will introduce a way to calculate the tidal velocity υ (i.e. tidal excursion E) and the tidal propagation celerity (c) using the analytical hydrodynamics models by Cai, et al. (2012) and Cai and Savenije (2013). However, without geometry and friction data at the estuary mouth, the analytical model for tidal dynamics cannot be used in this case. Therefore, the input parameters in this study are calibrated using the measurements of salinity. The calibration of the parameters are presented one by one in Section 4.1 in the revised version.

Cai, H., Savenije, H. H. G., and Toffolon, M.: A new analytical framework for assessing the effect of sea-level rise and dredging on tidal damping in estuaries, J. Geophys. Res., 117, C09023, doi:10.1029/2012JC008000, 2012.

Cai, H., and Savenije, H. H. G.: Asymptotic behavior of tidal damping in alluvial estuaries, J. Geophys. Res., 118(11), 6107-6122, https://doi.org/10.1002/2013JC008772, 2013.

4. In the application of the model to the Humen estuary, the first location of measurements (Dahu, figure 1) was set as the mouth of the estuary, and authors only calculated the results between station 1 and station 6 (figure 4). Actually, the real mouth is far downstream from station 1.

The Humen estuary is the largest river outlet in Lingding Bay that connects the South China Sea and the Humen estuary. In this study, we choose the Dahu station (station 1) as the mouth of the estuary because it is usually considered as the bayhead of the Lingding Bay (Liu et al., 2000; Tian, 1986). The Dahu station is the connection point between the Humen estuary and Lingding Bay.

Liu, P., Wen, P., Zhou, Z., and Yu, T.: Analysis of influencing factor on shoal and though development of Lingdingyang Bay at Zhujiang Estuary, Journal of Oceanography in Taiwan Strait, 2000, 19(1), 119-124.

Tian, X.,: A study on turbidity maximum in Lingdingyang Estuary of the Pearl River, Tropic Oceanology, 1986, 2.

5. In figure 2, the cross-sectional area of the Humen estuary was only shown for the reach between 0 km to 60 km. However, the Humen channel has a total length of 128 km (page 7, line 4). I think that the mouth in figure 2 should be the same as that in figure 4. If only part of the topography data was used, the area convergence length you obtained may be not correct. It is an important parameter in the model.

Unfortunately, this is all the cross-section information we have at our disposal. We agree it would be better to use a longer stretch of the channel to estimate convergence length, but at the same time we have no reason to believe the channel geometry would not fit the same function in the part where we have no geometry data.

6. Section 4.1 (Application to the Humen Estuary) is about calibration of model. Authors only discussed the calibration of parameters. The calibration results of model were shown in section 4.2 (model validation). In other words, model calibration and model validation used the same data. Although in figure 4 the results between 29 January and 3 February were shown, the conditions were similar.

We have rewritten Section 4.1 to clarify this in the revised version. The calibrated parameters include tidal excursion *E* and dispersion coefficient *D*. Although each of the calibrated dispersion coefficient from 29 January to 3 February was listed in Table 2, in fact, only the one on 29 January was used in the study. In other words, we use the data on 29 January to calibrate the model parameters, and use the data from 30 January to 3 February to validate the model. We agree it would be interesting to see how the model performs under different conditions. This contribution can be considered a proof of concept. In the revised version, we use two figures to show the results, Figure 4 is the calibrated result and Figure 5 is the validation results, as below:

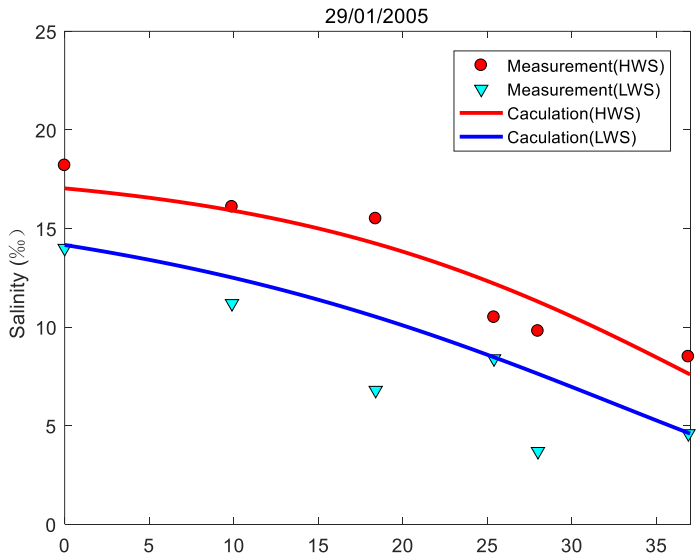

Figure 4: Comparison between calibration result and measured salinity concentration along the river on 29 January, 2005, showing values of measured salinity at high water slack (circle) and low water slack (inverted triangle), and the calibrated salinity curves at high water slack (red curve) and low water slack (blue curve).

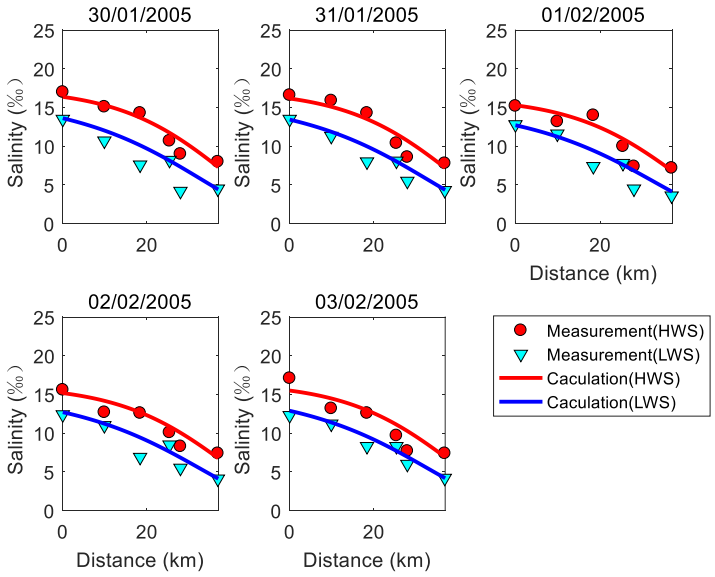

Figure 5: Comparison between validation result and measured salinity concentration along the river from 30 January to 3 February, 2005.

7. Section 6 Conclusions. In this manuscript, the main work is application of the model to the Humen estuary, showing calibration results. The first paragraph is enough. In the second paragraph, part is about results instead of conclusions, and the other part is already in the first paragraph. In addition, "predictive", "predicating", and "predictable" used in conclusions are not proper.

We appreciate the reviewer's suggestion and deleted this part of conclusions in the revised version.

Minor points:

1. Page 1, lines 16-17: "Compared with steady-state solutions, it can directly reflect the influence of the tide and the interaction between the tide and runoff". Salt intrusion is the result of interaction between tide and runoff. The steady-state solution cannot reflect the influence of tide and interaction of tide and runoff? And authors did not compare their solution with steady-state solutions.

We agree that the steady-state solution can reflect tidal influence and interaction of the tidal motion and runoff. We have modified that inaccurate description in the revised version as below:

"…It is derived from a one-dimensional advection-diffusion equation for salinity, adopting a constant mixing coefficient and a single-frequency tidal wave, which can directly reflect the influence of the tidal motion and the interaction between the tide and runoff…"

There are two reasons why we did not compare our solution with other steady models in this paper. Firstly, in this study, we concentrated more on analyzing and discussing the ability of our unsteady model to capture the intratidal variation of the salinity. Secondly, the steady-state solution of our model obtained by

integrating over the tidal period has the same expression as a widely used analytical model defined by Brockway et al. (2006). So, not surprisingly, our model applies well to the estimation of salinity distribution compared to the observations. Moreover, we did the relevant research and investigated the applicability of different steady solutions. Brockway's model has a simple calculation process and provides an accurate distribution of salinity in the downstream estuary (Xu et al., 2015).

Brockway, R., Bowers, D., Hoguane, A., Dove, V., and Vassele, V.: A note on salt intrusion in funnel–shaped estuaries: Application to the Incomati estuary, Mozambique, Estuarine Coastal Shelf Sci., 2006, 66, 1–5.

Xu, Y.W., Zhang, W., Chen, X.H., Zheng, J.H., Chen, X.W., Wu, H.X.: Comparison of Analytical Solutions for Salt Intrusion Applied to the Modaomen Estuary, J. Coastal Res., 2015, 31(3), 735-741.

2. Page 1, line 31 and page 2, line 1: "Hence, the effects of human activities on salt intrusion are of major interest to engineers and scientists". This sentence is not related to the topic of this manuscript. Authors did not do anything about the influence of human activities.

We appreciate the reviewer's suggestion and deleted this sentence in the revised version.

3. Page 3, lines 2-5. The sentences about paper organization are not necessary.

Agreed, we deleted this part of introduction in the revised version.

4. Page 6. What is e in equations 17 and 18?

***e* is the damping length of the tidal excursion. We explain this in the revised version as below:**

"…where *E*0 is the tidal excursion at the mouth (*x*=0), and *e* is the damping length of the tidal excursion…"

5. Page 6, line 20. Here the citation of a reference is not necessary. Particularly the reference is from a foreigner. Is a foreigner more familiar with a Chinese estuary?

We appreciate the reviewer's suggestion and deleted it in the revised version.

6. Page 7, line 6. What does the ES mean?

It was a mistake here. It should be "SE" which represents Southeast. We have corrected it in the revised version.

7. Page 7, lines 16-17: "The Humen waterway is well-mixed in the dry seasons (Luo et al., 2010)". The mixing condition can be seen directly from the vertical distribution of salinity, which should be shown in section 3.1 (overview of the study area).

The field survey was carried out by Guangdong Province Hydrology Bureau and the Pearl Hydrology Bureau from the River Conservancy Commission.

Unfortunately, they only provided us the vertical averaged salinity at each measuring location because of the well-mixed condition in Humen estuary. To justify the lack of the vertical salinity data, we add more citations to support the assumption of well-mixed conditions in the revised version, as below:
"…The Humen estuary is well-mixed under normal flow conditions during the dry season (Ou, 2009; Luo et al., 2010). Due to three years of drought, the river discharge decreased by 50 percent during the study period in 2005 compared to a normal year (Liao, Pan, and Dong, 2008). Thus, there is no doubt that well-mixed conditions prevailed during the calibration and validation…"

Liao, D.Y.; Pan, T.J., and Dong, Y.L., 2008. Characteristics of salt intrusion and its impact analysis in Guangzhou. Environment, S1, 4-5. (In Chinese)
Luo, L., Chen, J., Yang, W., and Wang, D.X, 2010. An intensive saltwater intrusion in the pearl river delta during the winter of 2007–2008, J. Trop. Oceanogr., 6, 22-28. (In Chinese)
Ou, S.Y., 2009. Spatial difference about activity of saline water intrusion in the Pearl River Delta. Scientia Geographica Sinica, 29(1), 89-92. (In Chinese)

8. Page 7, section 3.2 data. What data about the tide was used in this study? In line 12, it is tidal flow. But in line 19, it is tidal level.

The data of tidal flow is needed in our analytical solution, i.e. Eq (11). However, in this study, we used the tidal excursion instead of the tidal velocity, adopting a theoretical relation.

9. The title of section 4.1 can be changed into "Model calibration", corresponding with section 4.2 Model validation.

We appreciate the reviewer's suggestion and changed the title of section 4.1 into "Model calibration" in the revised version.

10. Page 9, lines 18-19. Why did you use the daily maximum and minimum salinity in figure 4?

Because the salinity were measured at hourly intervals. The daily maximum and minimum salinity were used as the approximate HWS and LWS salinity since the exact salinity values at HWS/LWS couldn't be obtained.

11. Page 9, the last paragraph. I did not understand what authors wanted to express except for the first sentence. In the first sentence, the "downstream" is relative to the 40 km reach in figure 4 or the whole channel? It can be seen from figure 4 that the main overestimates occur at station 3 and station 5.

Our study area is the downstream part of Humen estuary, therefore, "downstream" is relative to the whole channel. In Figure 4, we use 72 measured salinity observations at six stations at HWS and LWS to analyze the calculation results. As shown in Figure 4, overestimations occur at stations 2, 3, 4 and 5; 32 of the 72 measured salinity observations are overestimated compared with the

calculation results, while 8 are underestimated.

12. Page 10, line 16: "salinity variation is more symmetrical further away from the study site". What does this sentence mean? It is difficult to understand.

The sentence means: Farther away from the mouth, the calculation of the intertidal variation improves, featuring more symmetry in the tidal cycle.

13. Page 10, lines 29-30. Authors used this sentence to explain the nonperiodic variation of salinity at Machong station in figure 5. It seems that only in the second tidal cycle, the variation is abnormal.

In comparison with the calculation results at the other stations, the model doesn't perform very well in Machong station. This may relate to nonperiodic variation in the velocity signal.

14. Page 16, table 2. All parameters used in the model should be shown.

We appreciate the reviewer's suggestion. All parameters used in the model are shown in Table 3 in the revised version as below:

Table 3 Calibrated values of Parameters

Parameter	Unit	Value
A_0	m^2	37822
a	km	16.7
D	m^2/s	2562
E_0	km	26.7
e	km	30
c	m/s	12
φ_0	rad/s	-0.7

15. Page 17, figure 1.
(1) The Pearl River estuary is too complicated, and Humen is only one of eight branches. The figure caption is map of Humen estuary. But where is Humen? Only six gauging stations can be seen. The Humen estuary should be enlarged and shown clearly.
(2) River names "Beijiang River and Xijiang River" are different from the names "the North river and West river" in the text.
(3) East River and the Shiziyang channel in Page 10, line 23 were not shown in figure 1.

We appreciate the reviewer's suggestion and redraw Figure 1 in the revised version as below:

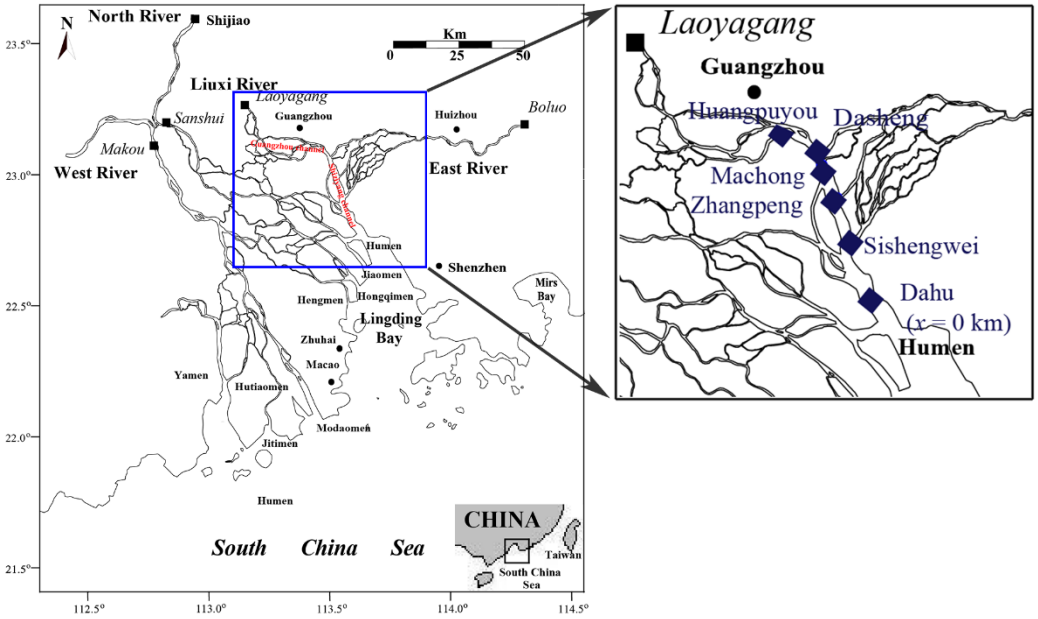

Figure 1: Map of the Humen estuary, showing the gauging stations where salinity concentration was measured during the field survey from 29 January to 3 February, 2005.

16. Page 19, caption of figure 3: "The linear relationship between these quantities predicted by Eq. (12) has been confirmed for all surveys, and the figures here show the linear line fitting results from Jan. 29th to Feb. 3rd". Page 22, caption of figure 6: "The subtidal discharge switches from seaward to landward between Machong and Dasheng stations, which will have an impact on salinity dynamics." These sentences should not be in the figure caption.

We appreciate the reviewer's suggestion and deleted them in the revised version.

17. The legends should be inside or outside figures, instead of covering the curves or words, such as figure 4, figure 6, and figure 7.

We redraw Figures 4, 6 and 7 in the revised version as below:

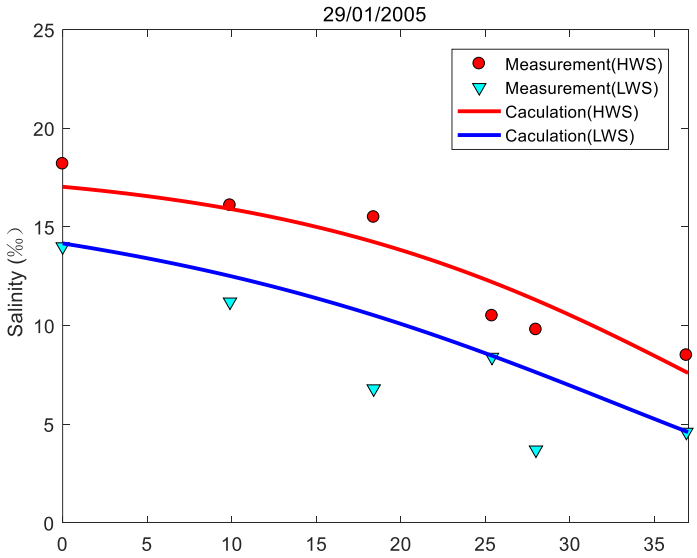

Figure 4: Comparison between calibration result and measured salinity concentration along the river on 29 January, 2005, showing values of measured salinity at high water slack (circle) and low water slack (inverted triangle), and the calibrated salinity curves at high water slack (red curve) and low water slack (blue curve).

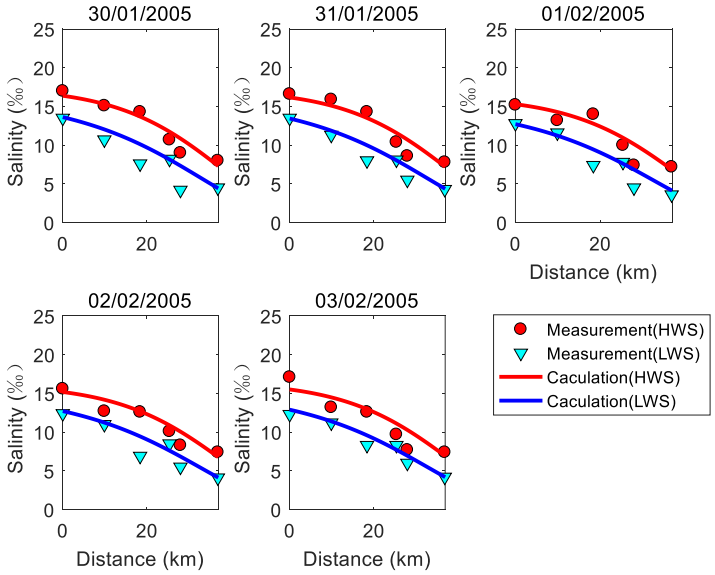

Figure 5: Comparison between validation result and measured salinity concentration along the river from 30 January to 3 February, 2005.

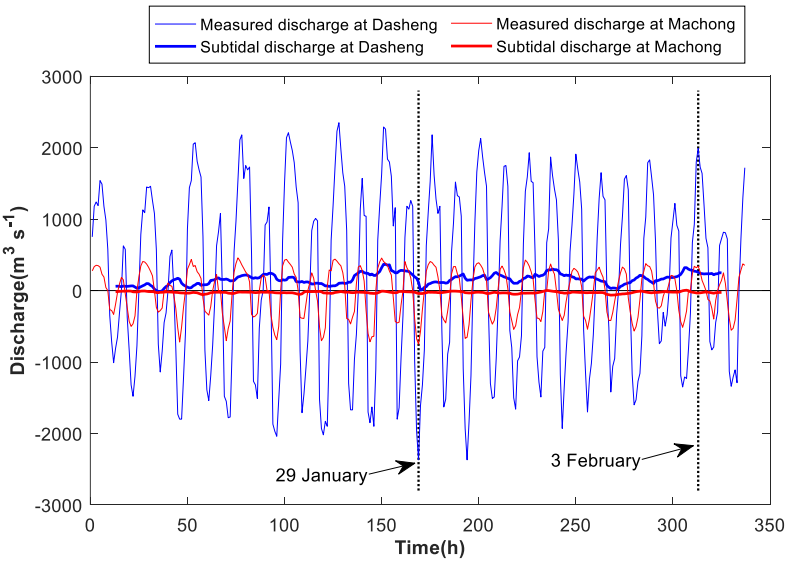

Figure 7: Subtidal discharge measured at Machong station and Dasheng station from 29 January through 3 February. Positive values mean seaward.

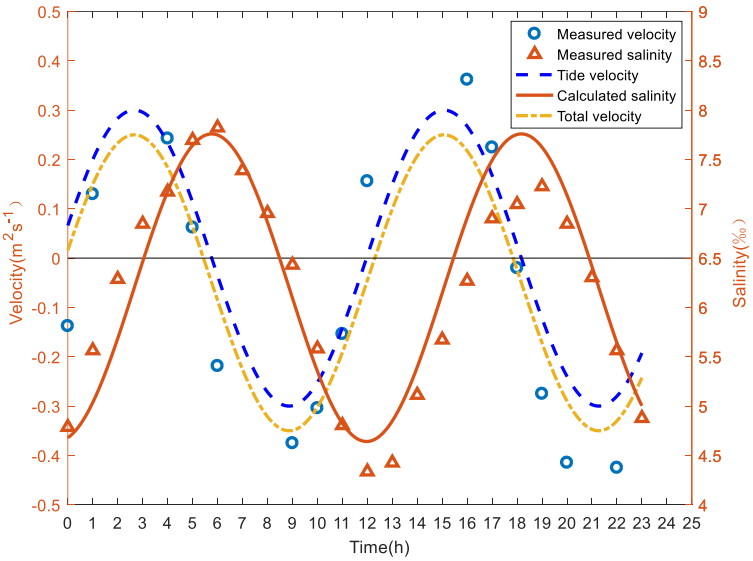

Figure 11: Salinity and tidal flow velocity over a tidal cycle at Huangpuyou station. The measured salinity is represented by triangles and the measured flow velocity is indicated by circles (on 31 January 2005). The dashes line is the calculated tidal velocity while the dash-dotted line is the total velocity of tidal flow and river flow. The red solid curve represents salinity simulated by the unsteady analytical solution, which reproduces the time lag HWS and maximum salinity.

18. Is Humen a waterway or estuary? In some figure and table captions waterway was used, but in others estuary was used. It is the same in the text.

It should be Humen estuary. We have corrected the in the revised version.

19. English writing should be improved. For examples:
(1) Page 7, line 19, "salinity was obtained by using a salimeter". "by" or "using" is

enough.
(2) Page 9 and page 10. "Analysis of " in the titles of section 4.2.1 and 4.2.2 can be deleted. They are not necessary.
(3) Page 12, line 8, "the predicted result obtained by this model". "predicted" or "obtained" is enough.
(4) Page 16, caption of table 2: "Values of the parameters of salt intrusion in Humen estuary". "Values of the" can be deleted, "parameters" is enough.
These are only examples. Authors should check every sentence to make them standard, concise, and fluency

We appreciate the reviewer's suggestion and have made efforts to improve the English grammar in the revised version.

Relevant changes made in the manuscript

1. In Section 1 of the revision, the existing unsteady state analytical model that we build upon is further introduced on Page 2 (Lines 29-33).

2. In Section 2, an alternative, analytical way to calculate the tidal excursion (E) and the tidal propagation celerity (c) is introduced on Page 6 (Lines 16-24). Although this analytical model is not directly applicable to our field case, and we consider it off-topic to elaborate on this, we do think it is worth pointing the readers to the possibility of this approach, which may be appropriate in different settings.

3. In Section 3.2, the measuring locations are clarified on Page 7 (Line 33) in the revised version. Moreover, we add more citations to support the assumption of well-mixed conditions on Page 8 (Lines 1-4) in the revised version.

4. In Section 4.1, the calibration of parameters is now clearly discussed on Page 9 (Lines 9-19). All the parameters used in the model are now presented in Table 3, and the calibration results of model are shown in Figure 4 of the revision.

5. In Section 4.2, our model results are compared with the previous model results on Page 11 (Lines 13-28), as shown in Figure 8 in the revision.

6. In Section 4.3, a sensitivity analysis is added, to discuss the impacts of the tidal and riverine forcing on the salinity variation on Page 12 (Lines 1-22), as shown in Figures 9 and 10 in the revised version.

7. In the new Figure 1, the Humen estuary is enlarged and all the locations that were mentioned in the main text are indicated.

8. In the new Figure 2, a logarithm scale is used.

9. In Figures 4, 5, 7 and 11, the legend is relocated to a more suitable place.

10. Based on the comments of reviewers, superfluous sentences are deleted and the English writing is improved.

Analytical model captures intratidal variation of salinity in a convergent, well-mixed estuary

Yanwen Xu[1, 2, 3], Antonius J. F. Hoitink[4], Jinhai Zheng[2, 5], Karl K ästner[4], Wei Zhang[2, 5]

[1] Key Laboratory of Coastal Disasters and Defense of Ministry of Education, Hohai University, Nanjing 210098, China
[2] College of Harbor, Coastal and Offshore Engineering, Hohai University, Nanjing 210098, China
[3] Key Laboratory of the Pearl River Estuarine Dynamics and Associated Process Regulation, Ministry of Water Resources, Guangzhou 510611, China
[4] Hydrology and Quantitative, Water Management Group, Department of Environmental Sciences, Wageningen University, The Netherlands
[5] State key laboratory of Hydrology-Water Resources and Hydraulic Engineering, Hohai University, Nanjing 210098, China

Correspondence to: Wei Zhang (zhangweihhu@126.com)

Abstract. Knowledge of the processes governing salt intrusion in estuaries is important since it influences the eco-environment of estuaries as well as its water resource potential in many ways. Analytical models of salinity variation offer a simple and efficient method to study salt intrusion in estuaries. In this paper, an unsteady analytical solution is presented to predict~~simulate~~ the spatial-temporal variation of salinity in convergent estuaries. It is derived from a one-dimensional advection-diffusion equation for salinity, adopting a constant mixing coefficient and a single-frequency tidal wave, which ~~. Compared with steady-state solutions, it~~ can directly reflect the influence of the tidal motion~~e~~ and the interaction between the tide and runoff. The deduced analytical solution is illustrated with an application to the Humen estuary of the Pearl River Delta (PRD), and proves to be an efficient and accurate approach to predict~~predicate~~ the salt intrusion in convergent estuaries. The unsteady analytical solution is tested against observations from~~six surveys made at~~ six study sites, to validate its capability to predict intratidal variation of salt intrusion~~of predicating salt intrusion variation~~. The results show that the proposed unsteady analytical solution can be successfully used to reproduce the spatial distribution and temporal processes governing salinity dynamics in convergent, well-mixed estuaries. The proposed method~~Meanwhile, this predictive equation~~ provides a quick and convenient approach to decide upon water fetching works to make good use of water resources.

1 Introduction

~~The s~~Salt intrusion in a river communicating with the~~a~~ sea is largely controlled by the river flow (Keulegan~~Keulegen~~, 1966). The salinity of estuary waters is the result of the balance between river and tidal fluxes, and mixing ~~in~~ between them. The natural variability of river and tidal inputs to estuaries has been greatly disrupted as a result of the impact of global climate change and sea level rise as well as of local human activities, such as dam construction and channel dredging. ~~of global climate change and human activities, such as sea level rise, dam construction and channel dredging.~~ These changes cause salt intrusion to become a serious problem in estuaries. It influences water quality, agricultural development in lowland areas, water

utilization in upstream catchments, and the aquatic environment in estuaries (Han et al., 2010; Mo et al., 2007; Savenije, 1992). ~~Hence, the effects of human activities on salt intrusion are of major interest to engineers and scientists.~~ To address this issue worldwide, research efforts devoted to salt intrusion have been conducted in laboratory tanks, with numerical models and using analytical approaches.

Nowadays, numerical models have become the most popular tool~~s~~ to study ~~the basic rules of~~ salinity distribution in estuaries, because they~~it~~ can provide visible results presenting the spatial-temporal variation in detail (e.g. Gong et al., 2012; Lerczak et al., 2006; MacCready, 2004; Wu and Zhu, 2010). However, the application of a numerical model is not an easy task since it requires detailed data of the bathymetry, and of hydrological boundary conditions~~and from hydrological variables~~, which are not available for all estuaries in the world. Here, a comparatively simple and convenient analytical model is developed as an efficient method to study the salt intrusion in well-mixed estuaries. Analytical models are widely used because they are ~~very~~ simple, while ~~still~~ retaining the basic physical characteristics involved. In the early 1960s, when systematic methods were developed to explore the factors controlling the instantaneous longitudinal salinity distribution, an expression was developed to compute the salt intrusion length as a function of the estuary length, mean depth, tidal amplitude, tidal period, fresh-water discharge, ocean salinity, and estuary roughness (Ippen and Harleman, 1961). In a subsequent period, analytical models of increasing complexity were developed based on the one-dimensional advection diffusion equation (Cameron and Pritchard, 1963), and on two-dimensional equations (Hansen and Rattray, 1965), capturing the dynamics of buoyancy driven exchange flow and tidal mixing, satisfying salt conservation. Since the 1970s, numerous empirical and semi-empirical one-dimensional analytical models were put forward that correlated the salt intrusion length to the estuarine dynamical conditions and geomorphology, based on the flume experiments and field measurements (e.g. Brockway et al., 2006; Fischer, 1974; Gay and O'Donnell, 2007, 2009; Kuijper and Rijn, 2011; Lewis and Uncles, 2003; Prandle, 1981, 1985; Rigter, 1973; Savenije, 1986). Although the literature on salt intrusion is vast, most studies concentrate on salt water intrusion~~salty water~~ in a prismatic flume for reasons of convenience. However, the majority of estuaries in the world converge in width ~~In the majority of real estuaries worldwide, however, the channels are convergent~~. The topography of the estuary is crucial to salt intrusion, because the two main drivers (i.e. river flow and the tidal motion) both depend on the topography. The cross-section area determines the amount of the salt water~~salty water~~ entering ~~into~~ the estuary, and the efficiency of fresh water carrying salt out of the estuary. Savenije (1986~~So, a~~A) developed a fully analytical and predictive model to predict salt intrusion that applies to the natural topography of alluvial estuaries ~~was developed to predictfor computation of salt intrusion (Savenije, 1986)~~. It has been well validated in numerous estuaries where the width converges ~~in an~~ exponentially ~~manner~~ ~~with the converging banks following an exponential function based on the field measurements~~ (e.g. Savenije, 1989; Savenije and Pagès, 1992; Nguyen and Savenije, 2006; Eaton, 2007; Ervine et al., 2007; ~~Nguyen and Savenije, 2006;~~ Nguyen et al., 2008~~; Savenije, 1989; Savenije and Pagès, 1992~~). In the years 2000-2010, another analytical approach (Brockway et al., 2006) was put forward, which can be considered as a modified and simplified version of the method presented in earlier studies (Prandle, 1981; Savenije, 1986). The dispersion coefficient in Brockway's model is assumed to be constant along the estuary, while it is assumed to be proportional to the subtidal axial velocity in Savenije's model. In the theoretical models ~~achievements~~ described above, ~~the vast majority of models described~~

~~above predict~~ the salt intrusion is predicted as a steady-state solution during slack water ~~the vast majority of researchers focus on the steady-state problem at a slack water~~. ~~There are f~~Few studies have focused on analyzing the intratidal variation of salinity analytically. Song et al. (2008) proposed an unsteady-state model applicable to laboratory flumes and artificial channels where the cross section is assumed to be constant along the channel. Elaborating on the work of Song et al. (2008), ~~Here~~here, an unsteady-state model is developed to predict~~simulate~~ the intratidal salinity intrusion dynamics in alluvial estuaries where the cross-section area typically converges~~, quantifying the peak intrusion length within a tidal cycle~~.

The aim of this study is to ~~obtain~~ introduce a simple, unsteady analytical solution to the problem of predicting the ~~spatial-temporal~~intratidal variation of salt intrusion in convergent, well-mixed estuaries. ~~This paper is organized as follows. The analytical model is introduced in Section 2, which is followed by the description of the study area in Section 3. In Section 4, the analytical solution is validated against field measurements of salt intrusion conducted in the Pearl River estuary. Subsequently, a discussion about the practical applications is presented in Section 5. The final section contains a summary and conclusions.~~

2 Methods

The cross-sectional area in this paper is described as an exponential function:

$$A = A_0 \exp(-x/a), \tag{1}$$

where A_0 is the cross-sectional area at the mouth (x=0), x is distance along the estuary and a is the convergence length of the cross-sectional area ~~which can be obtained by curve fitting of the cross-sectional areas~~. The x-axis has its origin at the mouth of the estuary and the upstream direction is taken as positive.

The one-dimensional advection-diffusion equation for salinity can be written as follows:

$$\frac{\partial As}{\partial t} + \frac{\partial Aus}{\partial x} = \frac{\partial}{\partial x}\left(AD\frac{\partial s}{\partial x}\right), \tag{2}$$

where s is salinity averaged over the~~a~~ cross-section, t is time, u is the velocity and D is the longitudinal dispersion coefficient. Although the assumption of a variable coefficient seems to be more reasonable, models with a constant dispersion coefficient have also proved to be capable of satisfactorily reproducing the salinity distribution (Lewis and Uncles, 2003; Brockway et al., 2006; Gay and O'Donnell, 2007, 2009~~; Lewis and Uncles, 2003~~). Under the assumption that D is independent of time, the salinity can be expanded in a Fourier series and be expressed as (Song et al., 2008):

$$s = \bar{s} + s_1\cos(\omega t + \varphi) + s_2\sin(\omega t + \varphi), \tag{3}$$

where $\bar{s}$ is the tidal-averaged salinity, s_1 and s_2 are coefficients. For the case of a simple harmonic wave with river discharge, the instantaneous flow velocity u is considered to consist of a time-dependent component $u_t = \upsilon\cos(\omega t + \varphi)$ created by the tide, and a steady component $u_f = Q_f / A$ contributed by the river flow:

$$u = u_f + \upsilon\cos(\omega t + \varphi), \tag{4}$$

where the value of the runoff velocity u_f is negative. Introducing Eqs. (3) and (4) into Eq. (2), and using $\theta = \omega t + \varphi$ yields:

$$\begin{aligned}&\left(u_f\frac{\partial s_2}{\partial x} - \omega s_1\right)\sin\theta + \left(\omega s_2 + u_f\frac{\partial s_1}{\partial x} + \upsilon\frac{\partial \bar{s}}{\partial x}\right)\cos\theta + u_f\frac{\partial \bar{s}}{\partial x} + \frac{\upsilon}{2}\frac{\partial s_1}{\partial x}\\ &= \left(D\frac{\partial^2 s_2}{\partial x^2} - \frac{D}{a}\frac{\partial s_2}{\partial x}\right)\sin\theta + \left(D\frac{\partial^2 s_1}{\partial x^2} - \frac{D}{a}\frac{\partial s_1}{\partial x}\right)\cos\theta + D\frac{\partial^2 \bar{s}}{\partial x^2} - \frac{D}{a}\frac{\partial \bar{s}}{\partial x},\end{aligned} \tag{5}$$

As the equation should hold for all values of θ, Eq. (5) yields the following set of equations:

$$\begin{cases}-\omega s_1 + u_f\dfrac{\partial s_2}{\partial x} = D\dfrac{\partial^2 s_2}{\partial x^2} - \dfrac{D}{a}\dfrac{\partial s_2}{\partial x},\\ \omega s_2 + u_f\dfrac{\partial s_1}{\partial x} + \upsilon\dfrac{\partial \bar{s}}{\partial x} = D\dfrac{\partial^2 s_1}{\partial x^2} - \dfrac{D}{a}\dfrac{\partial s_1}{\partial x},\\ u_f\dfrac{\partial \bar{s}}{\partial x} + \dfrac{\upsilon}{2}\dfrac{\partial s_1}{\partial x} = D\dfrac{\partial^2 \bar{s}}{\partial x^2} - \dfrac{D}{a}\dfrac{\partial \bar{s}}{\partial x},\end{cases} \tag{6}$$

where s, s_1 and s_2 can be further assumed as:

$$\begin{aligned}\bar{s} &= c_0\exp\left(m\left(\exp\left(\frac{x}{a}\right) - 1\right)\right),\\ s_1 &= c_1\exp\left(m\left(\exp\left(\frac{x}{a}\right) - 1\right)\right),\\ s_2 &= c_2\exp\left(m\left(\exp\left(\frac{x}{a}\right) - 1\right)\right),\end{aligned} \tag{7}$$

with $c_0 = \bar{s}_0$ is the tide-averaged salinity at the mouth of estuary.

Substitution of the equation set (7) into the equation set (6) yields:

$$\begin{cases}-\omega s_1 + \left(u_f + \dfrac{D}{a}\right)\dfrac{m}{a}\exp\left(\dfrac{x}{a}\right)s_2 = D\dfrac{m}{a}\exp\left(\dfrac{x}{a}\right)\left(\dfrac{1}{a} + \dfrac{m}{a}\exp\left(\dfrac{x}{a}\right)\right)s_2,\\ \omega s_2 + \upsilon\dfrac{m}{a}\exp\left(\dfrac{x}{a}\right)\bar{s} + \left(u_f + \dfrac{D}{a}\right)\dfrac{m}{a}\exp\left(\dfrac{x}{a}\right)s_1 = D\dfrac{m}{a}\exp\left(\dfrac{x}{a}\right)\left(\dfrac{1}{a} + \dfrac{m}{a}\exp\left(\dfrac{x}{a}\right)\right)s_1,\\ \left(u_f + \dfrac{D}{a}\right)\dfrac{m}{a}\exp\left(\dfrac{x}{a}\right)\bar{s} + \dfrac{\upsilon}{2}\dfrac{m}{a}\exp\left(\dfrac{x}{a}\right)s_1 = D\dfrac{m}{a}\exp\left(\dfrac{x}{a}\right)\left(\dfrac{1}{a} + \dfrac{m}{a}\exp\left(\dfrac{x}{a}\right)\right)\bar{s}.\end{cases} \tag{8}$$

Then, further elaboration yields:

$$\begin{cases} -\omega c_1 + \left(u_f - \dfrac{Dm}{a}\exp\left(\dfrac{x}{a}\right)\right)\dfrac{m}{a}\exp\left(\dfrac{x}{a}\right)c_2 = 0, \\ \omega c_2 + \upsilon\dfrac{m}{a}\exp\left(\dfrac{x}{a}\right)c_0 + \left(u_f - \dfrac{Dm}{a}\exp\left(\dfrac{x}{a}\right)\right)\dfrac{m}{a}\exp\left(\dfrac{x}{a}\right)c_1 = 0, \\ \left(u_f - \dfrac{Dm}{a}\exp\left(\dfrac{x}{a}\right)\right)\dfrac{m}{a}\exp\left(\dfrac{x}{a}\right)c_0 + \dfrac{\upsilon}{2}\dfrac{m}{a}\exp\left(\dfrac{x}{a}\right)c_1 = 0. \end{cases} \tag{9}$$

Hence, the solutions can be obtained:

$$\begin{cases} c_1 = \dfrac{\left(u_f - \dfrac{Dm}{a}\exp\left(\dfrac{x}{a}\right)\right)\dfrac{m}{a}\exp\left(\dfrac{x}{a}\right)}{\omega}c_2, \\ c_2 = \dfrac{-\upsilon\dfrac{m}{a}\exp\left(\dfrac{x}{a}\right)\omega}{\omega^2 + \left(u_f - \dfrac{Dm}{a}\exp\left(\dfrac{x}{a}\right)\right)^2\dfrac{m^2}{a^2}\exp\left(\dfrac{2x}{a}\right)}c_0, \\ m = \dfrac{u_f a\exp\left(-\dfrac{x}{a}\right)}{D} = \dfrac{Q_f a}{DA_0}. \end{cases} \tag{10}$$

The analytic solution of the unsteady state salinity distribution is therefore represented as:

$$s = \overline{s}_0\exp\left(\frac{Q_f a}{DA_0}\left(\exp\left(\frac{x}{a}\right)-1\right)\right)\left(1-\frac{\upsilon u_f}{\omega D}\sin\left(\omega t+\varphi\right)\right). \tag{11}$$

By integrating this unsteady salinity expression over the tidal period *T*, the salt intrusion under Tidal Average conditions (TA), as defined by Brockway et al. (2006), can be obtained as:

$$\overline{s}_x = \overline{s}_0\exp\left(\frac{Q_f a}{DA_0}\left(\exp\left(\frac{x}{a}\right)-1\right)\right). \tag{12}$$

A graph of the logarithm of salinity $\ln\left(\overline{s}/\overline{s}_0\right)$ against $\exp\left(x/a\right)$ should be a straight line, with the slope inversely proportional to the longitudinal dispersion coefficient *D* (Brockway et al., 2006). The coefficient *D* can then be calculated from:

$$D = \frac{Q_f a}{kA_0}, \tag{13}$$

where *k* is the slope of the fitted line. This approach makes it possible to estimate the longitudinal dispersion coefficient *D* based on the measurements of salinity made during a survey.

The tidal velocity amplitude υ can be estimated as $\upsilon = E\pi/T$ (Savenije, 1993) where E is the tidal excursion and the harmonic constant ω is given as $\omega = 2\pi/T$. Introducing $\upsilon = E\pi/T$ and $\omega = 2\pi/T$ into Eq. (11), and using $u_f = Q_f/A$ yields:

$$s = \bar{s}_0 \exp\left(\frac{Q_f a}{DA_0}\left(\exp\left(\frac{x}{a}\right)-1\right)\right)\left(1+\frac{E}{2a}\left(-\frac{Q_f a}{DA_0}\exp\left(\frac{x}{a}\right)\right)\sin(\omega t+\varphi)\right), \quad (14)$$

This expression can be used to describe the temporal and spatial variation of salinity, including High Water Slack (HWS) and Low Water Slack (LWS), when the tidal discharge is zero by definition. Since the maximum salinity is reached at HWS and the minimum salinity is reached at LWS (Savenije, 2005), Eq. (14) can be simplified for HWS into:

$$s_{\max} = \bar{s}_0 \exp\left(\frac{Q_f a}{DA_0}\left(\exp\left(\frac{x}{a}\right)-1\right)\right)\left(1+\frac{E}{2a}\left(-\frac{Q_f a}{DA_0}\exp\left(\frac{x}{a}\right)\right)\right), \quad (15)$$

and for LWS into:

$$s_{\min} = \bar{s}_0 \exp\left(\frac{Q_f a}{DA_0}\left(\exp\left(\frac{x}{a}\right)-1\right)\right)\left(1-\frac{E}{2a}\left(-\frac{Q_f a}{DA_0}\exp\left(\frac{x}{a}\right)\right)\right), \quad (16)$$

The tidal excursion E, the distance over which a water particle travels up and down the estuary with the flooding and ebbing tide, is assumed to decrease exponentially along the channel:

$$E = E_0 \exp(-x/e), \quad (17)$$

where E_0 is the tidal excursion at the mouth (x=0), and e is the damping length of the tidal excursion. Thus, combination of Eqs. (15), (16) and (17) yields:

$$E = \frac{a\left(s_{\max 0} - s_{\min 0}\right)}{\bar{s}_0\left(-\frac{Q_f a}{DA_0}\right)}\exp(-x/e), \quad (18)$$

where $s_{\max 0}$ is the maximum salinity at the estuary mouth and $s_{\min 0}$ is the minimum salinity at the estuary mouth. ~~After calibration of the parameters in Eq. (14), the spatial-temporal variation of the salinity distribution in estuaries is readily obtained.~~

Since the tidal flow is assumed ~~as~~to vary as a simple harmonic wave, the unsteady salinity model is here ~~is~~presented in its simplest form, with a single frequency. As the tidal propagation celerity in the estuary is assumed to be constant, the tidal phase at each site can be made up of an initial phase φ_0 at the mouth of the estuary and a phase difference that is the travel time of the tide from the mouth to the study site. Therefore, Eq. (14) can be modified as:

$$s = \bar{s}_0 \exp\left(\frac{Q_f a}{DA_0}\left(\exp\left(\frac{x}{a}\right)-1\right)\right)\left(1+\left(-\frac{E_0}{2a}\frac{Q_f a}{DA_0}\right)\exp\left(\frac{x}{a}-\frac{x}{e}\right)\sin\left(\omega\left(t-\frac{x}{c}\right)+\varphi_0\right)\right), \quad (19)$$

where c is the tidal propagation celerity.

We note that in the approach presented above the tidal excursion at the mouth is inferred from salinity data, whereas an alternative theoretical approach may be applicable that is less dependent on in situ data. T~~After calibration of the parameters in Eq. (14), the spatial temporal variation of the salinity distribution in estuaries is readily obtained.~~

~~T~~idal wave propagation can be described analytically by a set of four implicit equations (Cai et al., 2012), the phase lag equation $\tan(\varepsilon)=\lambda/(\gamma-\delta)$, the scaling equation $\mu=\sin(\varepsilon)/\lambda$, the damping equation $\delta=\gamma/2-4\chi\mu/(9\pi\lambda)-\chi\mu^2/3$, and the celerity equation $\lambda^2=1-\delta(\lambda-\delta)$, where λ is the celerity number $\lambda=c_0/c$, μ is the velocity number $\mu=\upsilon\bar{h}/(r_s\eta c_0)$, δ is the damping number $\delta=c_0\mathrm{d}\eta/(\eta\mathrm{d}x\omega)$, and ε is the phase lag between HW and HWS $\varepsilon=\pi/2-(\phi_Z-\phi_U)$. Here three dimensionless parameters control the tidal hydrodynamics (Savenije et al., 2008), i.e. the dimensionless tidal amplitude $\zeta=\eta/\bar{h}$, the estuary shape number $\gamma=c_0/(\omega a)$ and the friction number $\chi=r_s g c_0\zeta/\left(K_s^2\omega\bar{h}^{4/3}\right)\left[1-(4\zeta/3)^2\right]^{-1}$, where η is the tidal amplitude, K_S is the Manning-Strickler friction coefficient, r_s the storage width ratio, $\bar{h}$ is the tide-averaged depth and c_0 is the classical wave celerity $c_0=\sqrt{g\bar{h}/r_s}$.

Then with available geometry and friction data at the estuary mouth, the tidal propagation celerity and the tidal amplitude (or the tidal excursion) can be obtained by solving the set of four equations. Rather than proceeding with this analytical model for tidal hydodynamics, hereafter we employ Eq. 18 to close the set of equations.

3 Study area and data

3.1 Overview of study area

The Pearl River estuary (PRE) is located midway along the northern boundary of the South China Sea. It receives a large amount of fresh water from the Pearl River which has three major branches (i.e. the West River, the North River and the East River) in the upper drainage basin. The annual river discharge, with 80% occurring in the wet season, empties into the South China Sea via eight outlets (Zhao, 1990). The Lingding Bay is created by the inflows of freshwater from the Pearl River through four major discharge outlets, namely Humen, Jiaomen, Hongqimen, Hengmen. Historically, about 50-55% of the river flow enters the Lingding bay, while the remaining freshwater directly flows into the South China Sea through the four southwestern outlets (i.e. Modaomen, Jitimen, Hutiaomen and Yamen~~; Harrison et al., 2008~~).

The Humen is the largest river outlet in the Lingding bay and contributes 34.6% of the water discharge, i.e. about 603×10^8 m^3 in terms of annual water discharge (Ren et al., 2006). The freshwater input into Lingding bay through the Humen outlet comes from three sources: the East River, the Liuxi River and the North River. The annual river discharge with a peak of 1 870 m^3s^{-1}, measured at Niuxinling station in Liuxi River, is about 10 times less than that with a flood peak in excess of 12 000 m^3s^{-1}, measured in the other two rivers (Luo et al., 2002).

The tide in the Pearl River estuary has a mixed semidiurnal-diurnal character (Zhang et al., 2012). Among the eight outlets of the Pearl River estuary, Humen is most strongly dominated by the tide, with an annual average and maximum tidal range of 1.63 m and 2.59 m, respectively, at the mouth of the estuary (Li and Lei, 1998).

As a major tributary of the Pearl River, the Humen ~~channel~~estuary can be~~, has a total length of 128 km and is~~ divided into two waterways: the Guangzhou channel (the upper reach) with an average width of 431 m, and the Shiziyang channel (the lower reach) which is about 2200 m wide (Mai et al., 2001). It is a NW-~~ES~~ SE branch of the Pearl River estuary with a width of about 4 km at the mouth, ~~just like~~resembling an inverted funnel with a narrow neck in the north and a wide mouth opening to the south. The Humen outlet has the highest tidal prism in the Pearl River estuary due to the large-width of the mouth, resulting in a strong tidal motion. Especially, during spring tide in the dry season, when the river discharge is lowest, the downstream area becomes saline.

3.2 Data

The information available for the model application in this study includes data on topography, salinity, river discharge and on the tidal flow. A field survey for salt intrusion was conducted during the dry season in 2005. It was a project carried out by Guangdong Province Hydrology Bureau and the Pearl Hydrology Bureau from the River Conservancy Commission. In this paper, the field data from 29 ~~Jan.~~January ~~29th~~ to 3 ~~Feb.~~February ~~3rd~~ were used, which were measured at six gauge stations along the channel (~~Fig.~~Figure 1). Considering the impact of ~~the~~ shipping, the measuring positions were near the banks, with certain distances ranging from 605 m to 70 m. A Global Positioning System was used to confirm the exact measuring locations (Table 1). The Humen ~~waterway~~ estuary is well-mixed under normal flow conditions during the dry season~~in the dry seasons~~ (Ou, 2009; Luo et al., 2010). Due to three years of drought, the river discharge decreased by 50 percent during the study period in 2005 compared to a normal year (Liao, Pan, and Dong, 2008). Thus, there is no doubt that well-mixed conditions prevailed during the calibration and validation. The average salinity of vertical profiles was calculated based on the hourly water samples. At each location, the saline water was sampled at two different elevations: at 1/5 and 4/5 ~~times~~ of the depth of channel from the bed, and salinity was obtained ~~by~~ using a salimeter. ~~-~~The water discharge ~~and tidal levels~~ at stations ~~along the channel~~ were provided by the Hydrology Bureaus during the field survey. The cross-section was measured at mean sealevel, with the help of an ultrasonic echo-sounder.

Because of the complex river network upstream of the Humen area in the Pearl River estuary, the river discharge is difficult to determine. The total flux through the Humen outlet is composed of three parts which come from three main sources: the East River, the North River and the Liuxi River. The river discharge used in this paper was measured at upstream stations (Sanshui for the North River; Boluo for the East River and Laoyagang for the Liuxi River) from 29 ~~Jan.~~January ~~29th~~ to 3 ~~Feb.~~February ~~3rd~~. These data were collected from the official databases of the Hydrology Bureaus mentioned above. In the lower reach of the East River and the Liuxi River, respectively, Boluo station and Laoyagang station are located about 80 km upstream from the Humen outlet. The daily discharge measured at the Boluo station varied from 260 m^3s^{-1} to 400 m^3s^{-1} during the survey period, while it was about 20 m^3s^{-1} at the Laoyagang station. The discharge of the East River and the Liuxi River

entirely flow toward the Chinese sea through the Humen estuary ~~The discharge measured at the two stations (Boluo and Laoyagang) totally flowed into the South China Sea through the Humen outlet~~ (Ren et al., 2011). The North River is an important source for the river discharge to the Humen outlet. River discharge from the North ~~river~~ River reaches the Humen channel through a network of channels which connects to the western part of the Pearl River delta. Sanshui station is the primary hydrological station in the North River. About 11% of the measured discharge flows into the Humen estuary ~~was found to flow into the Humen channel~~ during the survey in 2005. Shanshui station is located further upstream than the other two stations (Boluo and Layaogang). The response lag of salinity variation at the estuary mouth to discharge variation at Sanshui station is about two~~2~~ days, while the river flow spends about one~~1~~ day to travel from Boluo and Laoyagang station to the estuary mouth.

4 Results

4.1 Model calibration ~~Application to the Humen Estuary~~

To demonstrate the practical application of the proposed analytical solution, the model has been used to simulate and analyze the spatial-temporal variation of salt intrusion in the Humen Estuary. In the following, the parameters of the analytical solution are obtained from calibration.

The spatial decay of the cross-sectional area of the Humen estuary can be described by the exponential function expressed in Eq. (1). The field data (triangles) and the best-fit line are shown in ~~Fig.~~Figure 2. The cross-sectional area at the mouth at mean tide, A_0, is calculated as 37 822 m^2 and the convergence length of cross section a is obtained by curve fitting as 16.7 km.

The relative salinity is plotted as $\ln(s/s_0)$ against $\exp(x/a)$ in ~~Fig.~~Figure 3. There is a straight line fit between these two variables, confirming the constancy of the dispersion coefficient. The dispersion coefficient D can be computed from the slope of the fitted lines~~.~~ ~~According~~ according to Eq. (12), ~~–~~where k is the slope. This approach has shown previously to be efficient (e.g. Brockway et al., 2006; Fang et al., 2006; Zhang et al., 2010). Table 2 shows the results of the fit for all these surveys carried out between 29 ~~Jan.~~January ~~29th~~ to 3 ~~Feb.~~February ~~3rd~~ (the slope in column 4 and the dispersion coefficient in column 6). The coefficient of determination (R^2) lies in the range between 0.85 and 0.92, with a mean value of 0.89. The assumption of the dispersion coefficient independent of distance is demonstrated to be reasonable and acceptable in the present case. The dispersion coefficient from data ~~from~~on 29 January is therefore used as the calibrat~~ion~~ed ~~parameter~~value ~~in this case~~.

~~In method section, an analytical hydrodynamics model is presented to reproduce the tidal excursion and the tidal propagation celerity. However, without geometry and friction data at the estuary mouth (or available water level recordings along an estuary), the analytical model for tidal dynamics cannot be used to estimate the tidal excursion in this case. Therefore, by means of the analytical model of salt intrusion based on the measurements of salinity,~~ ~~Thet~~The tidal excursion at the mouth of the estuary ~~can be~~is obtained through Eq. (18).

~~The tidal excursion can be approximated as the integral over time of the tidal velocity between the two moments of LWS and HWS. Considering it cumbersome to measure the tidal excursion directly by using boats, we present an approach to estimate~~

~~the tidal excursion by means of the analytical model of salt intrusion based on the measurements of salinity. The tidal excursion at the mouth of the estuary can be obtained through Eq. (18).~~For each tidal excursion at each day, the period-averaged value, maximum value and minimum value of salinity at the mouth are obtained by statistical analysis, and the longitudinal dispersion coefficient D is computed by ~~the~~ linear fitting, as shown previously. Moreover, the damping length of the tidal excursion e is calibrated using the observed salinity along the estuary. Similar to the tidal excursion, the value of the propagation celerity c is also obtained by calibration based on observations ~~since the analytical hydrodynamics model cannot be used without available data~~. The initial tidal phase φ_0 is calculated via a reverse procedure by calibration on the salinity at the mouth of estuary. Data from 31 January is used to verify the change of salinity over a tidal cycle.

The five calibration parameters (i.e. the convergence length of cross section a, the dispersion coefficient D, the tidal excursion E_0, the damping length of the tidal excursion e, the initial phase φ_0 and the tidal celerity c) are obtained based on the measurements at the mouth of the estuary, as shown in Table 3. Based on the observed data on 29 January, the results of the model calibration can be seen in Figure 4.

~~Since the tidal flow is assumed as a simple harmonic wave, the unsteady salinity model here is in its simplest form, with a single frequency. As the tidal propagation celerity in the estuary is assumed to be constant, the tidal phase at each site can be made up of an initial phase φ_0 at the mouth of the estuary and a phase difference that is the travel time of the tide from the mouth to the study site. Therefore, Eq. (14) can be modified as:~~

~~$$s = \bar{s}_0 \exp\left(\frac{Q_f a}{DA_0}\left(\exp\left(\frac{x}{a}\right)-1\right)\right)\left(1+\left(-\frac{E_0}{2a}\frac{Q_f a}{DA_0}\right)\exp\left(\frac{x}{a}-\frac{x}{e}\right)\sin\left(\omega\left(t-\frac{x}{c}\right)+\varphi_0\right)\right) \quad (19)$$~~

~~where c is the tidal propagation celerity. The initial tidal phase φ_0 is calculated via a reverse procedure by calibration on the observed salinity at the mouth of estuary. Additionally, the calibrated value of the propagation celerity is reliable and acceptable.~~

4.2. Model Validation

A validation of the unsteady model is offered in two separate parts, i.e. the longitudinal distribution of salinity along the channel and the temporal variation of salinity during the tidal period. In the first part, observations during two characteristic conditions (i.e. HWS and LWS) are chosen to validate against the calculated results of the salinity distribution. In the second part, a model for expressing the change process of salinity during tidal periods is established, according to the measurement on 31 ~~Jan.~~January. ~~31st.~~

4.2.1. L~~Analysis of l~~ongitudinal distribution of salinity

Based on the field measurements from 30 ~~Jan.~~January ~~29th~~ to 3 ~~Feb.~~February ~~3rd~~, Eqs. (15), (16) and (18) are used to calculate the longitudinal variation of salinity. Conditions of neap tide are considered to last from 31 January ~~31st~~ to 2 February ~~2nd~~.

The calibration results are presented in ~~Fig.~~Figure ~~5~~4. The good agreement between the computation and the measured data indicates that the performance of the unsteady analytical model is to a certain extent satisfactory in Humen estuary. The analytical model is found to better reproduce the distribution of salinity at high water (HW) than at low water (LW). This can be attributed to different degrees of mixing, which is stronger at HW. As the estuary is assumed to be well-mixed, the analytical model undoubtedly will perform better when mixing is higher. Fluctuations around the theoretical curve may partly be caused by the unequal distribution of salinity over the cross-section, or by the indirect derivation of the salinity at HWS and LWS, which is replaced with the daily maximum and minimum values, respectively.

It can be seen that the analytical model substantially overestimates the salinity in the downstream part of the estuary, partly because of the special locations of the stations (some are located at the confluence of rivers). The expression for the distribution analysis of salinity, Eq. (11), is multiplied the tidal average salinity with an extra component that reflects the effect of the tide and the interaction of the tide and river flow. This time-dependent component is a sine function, viz. $\left(-\upsilon u_f/\omega D\right)\sin(\omega t+\varphi)$, thus the calculated salinity at HWS and LWS is always symmetrical about the average values. The symmetry property of salinity has been demonstrated by Savenije (1989) under the assumption that the tidal excursion is independent of distance. After a transformation of variables, the sine function mentioned above is expressed as $\left(E/2a\right)(-Q_f a/DA)\sin(\omega t+\varphi)$ where the dispersion coefficient plays an important role. To simplify and clarify the interaction between the tidal motion and the river flow, the parameters D and Q_f are combined into one single calibration variable, the mixing coefficient α:

$$\alpha=-D/Q_f \text{ .} \tag{20}$$

which can be obtained in the same way as the dispersion coefficient. In this paper, the mixing coefficient is assumed constant along the channel, to develop a comparatively simple analytical solution within acceptable levels. It is calibrated by the measurements from Dahu station to Huangpuyou station, located at the junction of two reaches in the Humen estuary.

4.2.2. ~~Analysis of p~~Periodic variation of salinity

~~TData from Jan. 31 is used to verify the change of salinity over a tidal cycle. The calibration parameters (i.e. the tidal excursion E_0, the initial phase φ_0 and the tidal celerity c) are obtained based on the measurements at the mouth of the estuary. In addition,~~ the observations of salinity at hourly intervals along the Humen estuary are used to calibrate the dispersion coefficient in the model, and to analyze the change of salinity with time. The results indicate that the calibrated unsteady analytical model fits the observations well. ~~As shown in~~ ~~Fig.~~Figure ~~6~~5, where the analytical solution is compared with observation, ~~demonstrating~~ demonstrates that the proposed unsteady analytical solution is able to reflect the change process of salinity over a tidal cycle. Additionally, the simplification and assumption of the tidal celerity (c) and the initial phase at the mouth of estuary (φ_0) in Eq. (19) proves realistic.

The theoretical result of the periodic variation of salinity is not always consistent with the observations. As can be seen in ~~Fig.~~Figure ~~6~~5, the analytical model for simulating the temporal process of salinity has a relatively poor performance at the

sites near the mouth of estuary, such as Dahu station. By comparing the variation of salinity at different sites (~~Fig.~~Figure ~~6~~5), it shows that salinity variation is more symmetrical further away from the study site. The discrepancies near the mouth may have three reasons. Firstly, lateral residual circulation usually exists at the mouth of an estuary, where the cross section is widest. Secondly, the mouth of estuary is close to Lingding Bay, where the salt dynamics are influenced by coastal and ocean currents. Thirdly, near the outlet, comprehensive salinity measurements are much more difficult to take, due to the impact of tidal flats and complex hydrodynamics, influenced by Coriolis forcing and wind effects. All the influences above are related to the width of the channel, which gradually decreases in the landward direction.

The observations at Machong station show some nonperiodic variation, which may relate to the proximity of the confluence of the East River and the Shiziyang channel. At Dasheng station, about 2.6 km upstream from Machong station and near another confluence, the simulated temporal process of salinity shows a fairly good agreement with the observations. To understand the irregular changes of salinity at Machong station, the daily averaged discharges at Machong and Dasheng stations are analyzed by integrating over the tidal period. The results are presented in ~~Fig.~~Figure ~~6~~ 7 where the positive values represent the mean discharge transporting in the seaward direction. At Machong station, the mean discharge is directed inland, which can be attributed to Stokes transport (Buschman et al., 2010; Hoitink and Jay, 2016). At Dasheng station, only a few kilometers upstream, the mean discharge is seaward, as expected. The tide-averaged discharge thus converges in the estuary during low river flow, which will increase the total water volume in the estuary, and ~~creating~~ create a mean water level rise. We expect this process has an impact on the mean salt balance, which explains part of the observed discrepancies.

For comparison, the result obtained by Song's model is also presented here. The unsteady analytical model developed by Song et al. (2008) can reproduce the salinity process in an idealized estuary with constant depth and constant width, which is expressed as:

$$s = \bar{s}_0 \exp\left(\frac{u_f}{D_S}x\right)\left(1-\frac{u_f \upsilon}{D_S \omega}\sin(\omega t+\varphi)\right). \quad (21)$$

Therefore, in fact, it is more suitable for use in prismatic channels. The dispersion coefficient of Song's model is assumed to be independent on the distance, and can be estimated by:

$$D_S = -\frac{\bar{s}u_f \upsilon}{0.5\omega(s_{max}-s_{min})}. \quad (22)$$

When ~~A~~an estimation for tidal velocity is made according to the relation $\upsilon = E\pi/T$, and the value of the runoff velocity is obtained using $u_f = Q_f/A$, then the dispersion coefficient can be calculated based on the measured salinity at the mouth of the estuary. The data which has been used for modelling in Humen estuary can be found in Table 4. As shown in Figure 8, the performance of Song's model for the Humen estuary is satisfactory at the study sites close to the estuary mouth, e.g. the Dahu station and the Sishengwei station. However, the salt intrusion is underestimated by the model at the Zhangpeng station (Figure 8c) and the Dasheng station (Figure 8d), in the upstream part of the estuary. A ~~possible~~likely reason for the underestimation

can be the fundamental assumption that the channel has a constant cross section. The river ~~banks~~width convergence at the Humen estuary can actually be described by an exponential function. Simplifying this estuary geometry can result in the underestimation of the mixing coefficient. It indicates that topography is a key driver of the salt intrusion along the Humen estuary.

4.3. Sensitivity analysis

The amplitude of salinity can be described by:

$$\hat{s} = \overline{s}_x * I_s , \quad (23)$$

where $\overline{s}_x$ is the tide-averaged salinity along the estuary and is a function of the river discharge, i.e. Eq.(12). The parameter I_s is the salinity amplitude coefficient that is defined as:

$$I_s = -\frac{EQ_f}{2DA} , \quad (24)$$

representing the interaction between ~~the~~ tides and the river discharge. To investigate the longitudinal salinity distribution and intratidal salinity variation for different discharge and tidal dynamic conditions in the Humen estuary, Eqs. (12) and (23) are used to plot the longitudinal salinity curve and intratidal variation of salinity, respectively. The implemented parameters are the same as shown in Table 3, only the river discharge and the tidal excursion are variable.

Three constant discharge values of 200, 600 and 1800 m^3/s are used to evaluate the impact of the river discharge on the salinity variation. The discharge values are chosen because the minimum discharge in the dry season is around 600 m^3/s in the Humen estuary, and low salinity can be measured at Huangpuyou station when the discharge is larger than 1800 m^3/s. In addition, the discharge in the extreme dry season is set to be 200 m^3/s. The longitudinal salinity curve can be seen Figure 9a. At tidal average conditions, the salt intrusion length ~~gets~~becomes smaller when the discharge increases. The steepest salinity gradient can be found at the highest discharge (Q_f=1800 m^3/s). It is clear from Figure 9b that the salinity amplitude increases firstly and then decreases as the river discharge increases. This is because during periods of low river discharge (Q_f= 200 m^3/s), the tide-averaged salinity is larger but the salinity amplitude coefficient I_s is smaller, which indicates the weaker interaction between the river flow and the tides. However, the tide-averaged salinity decreases rapidly with the increasing river discharge, as we can see from Figure 9a, resulting in a smaller amplitude of salinity during periods of high river discharge (Q_f= 1800 m^3/s).

The tidal effect is studied using three different tidal excursions. The tidal excursion values result in the plots that is shown in Figure 10. The longitudinal salinity distribution at tidal average conditions is independent of the tidal excursion as can be seen in Figure 10a. From Eq. (23), since the salinity amplitude coefficient I_s is in direct proportion to the tidal excursion, the amplitude of the salinity shows a linearly increasing trend with the increased tidal excursion (Figure 10b).

5. Discussions

5.1. Time lag between salinity extremes and slack water

In estuaries, it is noticed that the maximum salinity appears after HWS and the minimum salinity appears before LWS. However, often, the salinity at HWS and LWS correspond approximately to the maximum and minimum salinity, respectively. But often, the salinity at HWS (or LWS) is approximated by with the maximum (or minimum) salinity, because it is hard to determine the exact value at HWS (or LWS) based on records of salinity. The accuracy of this approximation cannot be inferred from existing steady-state models for salt intrusion, as time variation is neglected. As shown in Fig.Figure 117, the unsteady analytical solution proposed in this paper demonstrates that the phase lag between tidal velocity and salinity transportation is $\pi/2$, which means that the extreme values of salinity appear when the tidal velocity is zero. Our unsteady equation for salinity (i.e. Eq. 11) demonstrates the influence of the river discharge on the occurrence of maximum and minimum salinity relative to HWS and LWS, respectively.

More generally, Eq. (14) offers a simple expression yielding qualitative insight into the role of the river discharge in the spatiotemporal variation of salinity in a well-mixed estuary. The time lag between salinity extremes and slack water is determined by the strength of the river flow, in a way that is consistent with the previous observations that the maximum salinity appears after HWS and the minimum salinity appears before LWS. The estimated river flow velocity at Huangpuyou station is about 1/6 of the tidal flow amplitude, resulting in a time lag between HW (at maximum salinity) and HWS (when total velocity is zero) of less than 30 minutes. At this station, it is acceptable to assume that the salinity reaches the maximum value at HWS and the minimum value at LWS.

5.2. Optimizing water intake

Estuaries are crucial feeding and breeding grounds for many life forms, and are a source of serve to supply drinking water. Intrusion of salt water can temporarily halt the production of drinking water, and put stress on plant and animal species that have adapted to the typical salt concentrations along Because of the various survival needs of estuarine flora and fauna, different species have different salinity demands, and salinity may frustrate the production of drinking water. the estuary. In China, a value of 0.5 ‰ of salinity is considered as the upper limit of drinking water (SWEQ PRC, 2002), while turbot farmed in man-made ponds need to live in the water with less than 12 ‰ of salinity. The unsteady solution proposed in this paper shows to reproduce the intratidal variation of salt intrusion, which allows to estimate the window of opportunity for drinking water intake, and has the potential of application in aquaculture and water fetching works in estuaries.

Due to the serious increase of salt intrusion in recent years, the water intake from Humen estuary is more suitable for saline-water aquaculture rather than the residential use. However, the salinity along the estuarine channel is changing all the time according to the variations of the tides as well as the freshwater discharge. This makes it important to capture the temporal variation of salinity for optimizing the water intake of the man-made ponds around the estuary. The analytical model proposed

in this study provides a simple and efficient approach to predicate the variation of salinity, which is economical and practical, with the limited amount of data available.

Close to Dasheng station, there is an aquaculture area with many man-made ponds of different sizes. Optimizing water intake is a key issue here. The ~~practicability~~applicatibity of the analytical model is ~~analyzed by~~ illustrated~~ing~~ by focussing on ~~its availability of~~ turbot farming ~~,with~~ which ~~required~~ requires salinity of no less than 12‰. The observed salinity data on 29 ~~Jan.~~January ~~29th~~ is used to calibrate the model, where the determination of three parameters is needed, i.e. tide~~al~~-averaged salinity at mouth $\overline{s}_0$, the slope ~~(~~ $k = \left(Q_f a / DA_0\right)$ ~~)~~ and the tidal excursion E. The decreasing trend of subtidal salinity is close to a linear relation from 29 ~~Jan.~~January ~~29th~~ to 3 ~~Feb.~~February ~~3rd~~ (~~Fig.~~Figure 12~~8~~b). Thus the tide~~al~~-averaged salinity value of the predicted model is set as 90% of that on 29 ~~Jan.~~January ~~29th~~, considering the slight change of the subtidal salinity in the five days after 29 ~~Jan.~~January ~~29th~~. Moreover, the slope as well as the tidal excursion are assumed to be constant during the whole period from 29 ~~Jan.~~January ~~29th~~ to 3 ~~Feb.~~February ~~3rd~~. As shown in ~~Fig.~~Figure 12~~8~~c, the prediction by the model ~~the predicted result obtained by this model~~ is in good agreement with the observation~~measured data~~ in this case. Furthermore, if more observed data is available to calibrate the tide~~al~~-averaged salinity covering the period from 29 ~~Jan.~~January ~~29th~~ to 3 ~~Feb.~~February ~~3rd~~, Eq. (14) performs better~~,appears to perform better~~ as shown in ~~Fig.~~Figure 12~~8~~d. The available time for water intake can be obtained from the prediction~~calculation results~~, when the salinity concentration~~salinity of water~~ reaches a value higher than 12 ‰.

Since the fresh water discharge influences the slope ~~exerts a control on the variation of the slope~~ (Brockway et al., 2012), it is reasonable to assume that the slope remains constant in a short time scale since the fresh water discharge variation has a time scale of days to months (~~Fig.~~Figure 12~~8~~a). The tidal excursion is the integral over time of the tidal velocity between the low water slack and high water slack. It varies from day to day as the tidal wave changes from neap tide to spring tide (Savenije, 2005). Therefore, the tidal excursion is assumed to be independent of time in the neap cycle from 29 ~~Jan.~~January ~~29th~~ to 3 ~~Feb.~~February ~~3rd~~. Besides, Equation (18) is demonstrated to be a useful equation for the calculation of the tidal excursion, which offers an approach to estimate the tidal excursion with salinity data. The predicted salinity fits well with observed values, indicating that the estimation of the tide~~al~~-averaged salinity during the neap tide is acceptable. However, the prediction accuracy of the model can be higher if more observed tide~~al~~-averaged salinity data is available.

6. Conclusions

An unsteady-state analytical solution of salt intrusion is proposed based on the one-dimensional advection-diffusion equation for salinity, assuming a harmonic tidal wave with a single-frequency and a constant mixing coefficient. The predictive skill of the model has been illustrated from an application to the Humen Estuary, which shows it can offer an efficient approach to ~~predicating~~ calculating the variation of salinity in a ~~convergent,~~ well-mixed estuary where the channel area is convergent. The

results show that the analytical model is able to reproduce the intratidal variation of salt intrusion, and can be a useful tool to compute the time windows in which salinity remains below a critical threshold in an estuary.

~~The influences of the tide and river discharge are adequately reflected in the analytical expression. The longitudinal salinity distributions at two characteristic conditions (i.e. HWS and LWS) were computed for validation. The results indicate that the analytical model can be an efficient and predictable approach if the constant mixing coefficient assumption holds. The salinity dynamics at six study sites has been simulated by the unsteady model based on the measurements and the calibrated parameters (i.e. tidal celerity and phase) at the mouth of estuary. The results compared favorably with the outcome of the analytical model. In summary, the unsteady state analytical model has been quantitatively evaluated by using the field data of Humen Estuary and demonstrated to be a predictive and efficient approach to describe the spatial temporal variation of salt intrusion in a convergent, well mixed estuary.~~

Author contributions

YX and WZ formulated the overarching research goals and aims. YX, AH and WZ contributed to the development of the methodology. YX, AH, JZ and WZ discussed and interpreted the results. YX created the figures and wrote the original draft. AH, JZ, KK and WZ reviewed and edited the draft.

Competing interests

The authors declare no competing interests.

Acknowledgement

This work was supported by the "National Key R&D Program of China" [grant numbers 2017YFC0405900], the "Fundamental Research Funds for the Central Universities" [grant numbers 2018B56214, 2017B21514, 2018B13114], the "National Natural Science Foundation of China" [grant numbers 41676078, 41506100], the "Open Foundation of Key Laboratory of Coastal Disasters and Defense of Ministry of Education" [grant numbers 201704] the "China Postdoctoral Science Foundation" [grant numbers 2017M621611], the "Open Research Foundation of Key Laboratory of the Pearl River Estuarine Dynamics and Associated Process Regulation, Ministry of Water Resources" [grant numbers 2018KJ05, 2017KJ04], and the "Project of Jiangsu Provincial Six Talent Peaks" [grant numbers XXRJ-008]. We thank the editor, Prof. Savenije, Dr. Cai and an anonymous reviewer for constructive comments on the initial draft of this manuscript.

References

Brockway, R., Bowers, D., Hoguane, A., Dove, V., and Vassele, V.: A note on salt intrusion in funnel–shaped estuaries: Application to the Incomati estuary, Mozambique, Estuarine Coastal Shelf Sci., 66, 1–5, doi:10.1016/j.ecss.2005.07.014, 2006.

Buschman, F. A., Hoitink, A. J. F., Van Der Vegt, M., and Hoekstra, P.: Subtidal flow division at a shallow tidal junction, Water Resour. Res., 46, doi: 10.1029/2010WR009266, 2010.

Cai, H., Savenije, H. H. G., and Toffolon, M.: A new analytical framework for assessing the effect of sea-level rise and dredging on tidal damping in estuaries, J. Geophys. Res., 117, C09023, doi:10.1029/2012JC008000, 2012.

Cameron, W. M. and Pritchard, D. W.: Estuaries, In: The Sea vol. 2, edited by: Hill, M. N., John Wiley and Sons, New York, USA, 306–324, 1963.

Eaton, T. T.: Analytical estimates of hydraulic parameters for an urbanized estuary–Flushing Bay, J. Hydrol., 347, 188–196. doi:10.1016/j.jhydrol.2007.09.018, 2007.

Ervine, D. A., Bekic, D., and Glasson, L.: Vulnerability of two estuaries to flooding and salinity intrusion, Water Sci. Technol. Water Supply, 7, 125–136, doi:10.2166/ws.2007.047, 2007.

Fang, L. G., Chen, S. S., Li, H. L., Zhang, L. X., Wang, J. F., and Zhang, H. O.: The establishment of GIS based simulation model of saltwater intrusion in Pearl River estuary, South China, in: Proceedings of 2006 IEEE International Symposium on Geoscience and Remote Sensing, Denver, CO, USA, 31 July–4 August, 2911–2914, 2006.

Fischer, H. B.: Discussion of 'Minimum length of salt intrusion in estuaries' by B. P. Rigter, 1973, J. Hydraul. Div. Proc., 100, 708–712, 1974.

Gay, P., and O'Donnell, J.: A simple advection–dispersion model for the salt distribution in linearly tapered estuaries, J. Geophys. Res., 112, C07021, doi:10.1029/2006JC003840, 2007.

Gay, P., and O'Donnell, J.: Comparison of the salinity structure of the Chesapeake Bay, the Delaware Bay and Long Island Sound using a linearly tapered advection–dispersion model, Estuaries Coasts, 32, 68–87, doi:10.1007/s12237-008-9101-4, 2009.

Gong, W., Wang, Y., and Jia, J.: The effect of interacting downstream branches on saltwater intrusion in the Modaomen Estuary, China, J. Asian Earth Sci. 45, 223–238, doi:10.1016/j.jseaes.2011.11.001, 2012.

Han, Z. Y., Tian, X. P., and Liu, F.: Study on the causes of intensified saline water intrusion into Modaomen Estuary of the Zhujiang River in recent years, J. Mar. Sci., 28, 52–59, doi:10.3969/j.issn.1001-909X.2010.02.007, 2010. (In Chinese)

Hansen, D. V. and Rattray, M.: Gravitational circulation in straits and estuaries, Issue 166 of Technical report, Department of Oceanography, University of Washington, USA, 19 pp., 1965.

Harrison, P. J., Yin, K., Lee, J. H. W., Gan, J., and Liu, H.: Physical–biological coupling in the Pearl River Estuary, Cont. Shelf Res., 28, 1405–1415, doi:10.1016/j.csr.2007.02.011, 2008.

Hoitink, A. J. F. and Jay, D. A.: Tidal river dynamics: Implications for deltas, Rev. Geophys., 54, 240–272, doi:10.1002/2015RG000507, 2016.

Ippen, A.T., and Harleman, D. R. F.: One dimensional analysis of salinity intrusion in estuaries, Technical Bulletin No. 5, Committee on Tidal Hydraulics, Waterways Experiment Station, Vicksburg, Mississippi, 69 pp., 1961.

Keulegan, G. H.: The mechanism of an arrested saline wedge, Estuary and coastline hydrodynamics, 546–574, 1966.

Kuijper, K., and Van Rijn, L. C.: Analytical and numerical analysis of tides and salinities in estuaries; part II: salinity distributions in prismatic and convergent tidal channels, Ocean Dyn., 61, 1743–1765, doi:10.1007/s10236-011-0454-z, 2011.

Lerczak, J. A., Geyer,W. R. and Chant, R. J.: Mechanisms driving the time–dependent salt flux in a partially stratified estuary, J. Phys. Oceanogr., 36, 2296–2311, doi:10.1175/JPO2959.1, 2006.

Lewis, R. E. and Uncles, R. J.: Factors affecting longitudinal dispersion in estuaries of different scale, Ocean Dyn., 53(3), 197–207, doi:10.1007/s10236-003-0030-2, 2003.

Li, C. C. and Lei, Y. P.: On the property and maintenance of the tidal channel of the Pearl River system from Guangzhou city to the Humen inlet, Trop. Geogr., 18, 24–28, doi:10.3969/j.issn.1001-5221.1998.01.005, 1998. (In Chinese)

Liao, D. Y., Pan, T. J., and Dong, Y. L.: Characteristics of salt intrusion and its impact analysis in Guangzhou. Environment, S1, 4-5, 2008. (In Chinese)

Luo, L., Chen, J., Yang, W., and Wang, D. X.: An intensive saltwater intrusion in the pearl river delta during the winter of 2007–2008, J. Trop. Oceanogr., 6, 22–28, doi: 10.1080/09500340.2010.529951, 2010. (In Chinese)

Luo, X. L., Yang, Q. S., and Jia, L. W.: Riverbed evolution of the Pearl River Delta, Sun Yat–Sen University Press, Guangzhou, China, 213 pp., 2002. (In Chinese)

MacCready, P.: Toward a unified theory of tidally–averaged estuarine salinity structure, Estuaries Coasts, 27, 561–570, doi:10.1007/BF02907644, 2004.

Mai, B. X., Fu, J. M., Zheng, G., Ling, Z., Min, Y. S., Sheng, G. Y., and Wang, X. M.: Polycyclic aromatic hydrocarbons in sediments from the Pearl River and estuary, China: spatial and temporal distribution and sources, Appl. Geochem., 16, 1429–1445, doi:10.1016/S0883-2927(01)00050-6, 2001.

Mo, S. P., Li, Y., and Lu, S. L.: Analysis of factors affecting saline water intrusion in Guangzhou waterway, Hydro–Sci. Eng., 4, 37–42, doi:10.16198/j.cnki.1009-640x.2007.04.001, 2007. (In Chinese)

Nguyen, A. D. and Savenije, H. H. G.: Salt intrusion in multi–channel estuaries: a case study in the Mekong Delta, Vietnam, Hydrol. Earth Syst. Sci., 10, 743–754, doi:10.5194/hess-10-743-2006, 2006.

Nguyen, A. D., Savenije, H. H. G., Pham, D. N., and Tang, D. T.: Using salt intrusion measurements to determine the freshwater discharge distribution over the branches of a multi–channel estuary: The Mekong Delta case, Estuarine Coastal Shelf Sci., 77, 433–445, doi:10.1016/j.ecss.2007.10.010, 2008.

Ou, S. Y.:. Spatial difference about activity of saline water intrusion in the Pearl River Delta, Scientia Geographica Sinica, 29(1), 89-92, doi:10.3969/j.issn.1000-0690.2009.01.014, 2009. (In Chinese)

Prandle, D.: Salinity intrusion in estuaries, J. Phys. Oceanogr., 11, 1311–1324, doi: 10.1175/1520-0485(1981)011<1311:SIIE>2.0.CO;2, 1981.

Prandle, D.: On salinity regimes and the vertical structure of residual flows in narrow tidal estuaries, Estuarine Coastal Shelf Sci., 20, 615–635, doi:10.1016/0272-7714(85)90111-8, 1985.

Ren, F. P., Jiang, Y., Xiong, X., Dong, M. Y., and Wang, B.: Characteristics of the Spatial–Temporal Differences of Land Use Changes in the Dongjiang River Basin from 1990 to 2009, Resour. Sci., 33, 143–152, 2011. (In Chinese)

Ren, J., Wu, C., and Bao, Y.: Dynamic structure of Humen estuary of the Pearl River, Acta Sci. Nat. Univ. Sun Yat-sen, 45, 105–109, doi:10.3321/j.issn:0529-6579.2006.03.026, 2006. (In Chinese)

Rigter, B. P.: Minimum length of salt intrusion in estuaries, J. Hydraul. Div. Proc., Proceedings of ASCE, 99, 1475–1496, 1973.

Savenije, H. H. G. and Pagès, J.: Hypersalinity: a dramatic change in the hydrology of Sahelian estuaries, J. Hydrol., 135, 157–174, doi:10.1016/0022-1694(92)90087-C, 1992.

Savenije, H. H. G.: A one–dimensional model for salinity intrusion in alluvial estuaries, J. Hydrol., 85, 87–109, doi:10.1016/0022-1694(86)90078-8, 1986.

Savenije, H. H. G.: Salt intrusion model for high–water slack, low–water slack, and mean tide on spread sheet, J. Hydrol., 107, 9–18, doi:10.1016/0022-1694(89)90046-2, 1989.

Savenije, H. H. G.: Rapid Assessment Technique for Salt intrusion in alluvial estuaries, Ph.D. thesis, International Institute for Infrastructural, Hydraulic and Environmental Engineering, Delft, The Netherlands, 203 pp., 1992.

Savenije, H. H. G.: Composition and driving mechanisms of longitudinal tidal average salinity dispersion in estuaries, J. Hydrol., 144, 127–141, doi:10.1016/0022-1694(93)90168-9, 1993.

Savenije, H. H. G.: Salinity and Tides in Alluvial Estuaries, Elsevier, Amsterdam, 197 pp., 2005.

Savenije, H. H. G., Toffolon, M., Haas, J., Veling, E. J. M.: Analytical description of tidal dynamics in convergent estuaries. J. Geophys. Res., 113(C10), C10025, doi:10.1029/2007JC004408, 2008.

Song, Z. Y., Huang, X. J., Zhang, H. G., Chen, X. Q., and Kong, J.: One–dimensional unsteady analytical solution of salinity intrusion in estuaries, China Ocean Eng., 22, 113–122, 2008.

Wu, H. and Zhu, J.: Advection scheme with 3rd high–order spatial interpolation at the middle temporal level and its application to saltwater intrusion in the Changjiang Estuary, Ocean Model., 33, 33–51, doi:10.1016/j.ocemod.2009.12.001, 2010.

Zhang, W., Feng, H., Zheng, J., Hoitink, A. J. F., van der Vegt, M., Zhu, Y., and Cai, H.: Numerical Simulation and Analysis of Saltwater Intrusion Lengths in the Pearl River Delta, China, J. Coastal Res., 29, 372–382, doi: 10.2112/JCOASTRES-D-12-00068.1, 2012.

Zhang, Z., Cui, B., Zhao, H., Fan, X., and Zhang, H.: Discharge–salinity relationships in Modaomen waterway, Pearl River estuary, Procedia Environ. Sci., 2, 1235–1245, doi: 10.1002/clen.201100735, 2010.

Zhao, H. T.: Evolution of the Pearl River estuary, China Ocean Press, Beijing, China, 116–147, 1990. (In Chinese)

TABLES

Table 1 General information of hydrological stations in the Humen waterway

Station name	Distance from the estuary mouth (km)	x-coordinate(m) *	y-coordinate(m) *
Dahu	0	2524802	38459960
Sishengwei	9.9	2534512	38458163
Zhangpeng	18.4	2542539	38455607
Machong	25.4	2548948	38452466
Dasheng	28.0	2551430	38451984
Huangpuyou	36.9	2553758	38443358

* The coordinate system's origin is set at 22°05'12.9894"N, 113°27'34.9899"E.

Table 2 Dispersion coefficient ~~Values of the parameters~~ of salt intrusion in Humen estuary

Data	River discharge Q_f (m^3/s)	Tide range H (m)	Slope k	R^2	Dispersion coefficient D (m^2/s)
29/01/2005	667	2.26	-0.115	0.85	2562
30/01/2005	626	2.05	-0.114	0.86	2425
31/01/2005	663	1.68	-0.118	0.92	2481
01/02/2005	705	1.43	-0.125	0.88	2492
02/02/2005	655	1.38	-0.108	0.92	2678
03/02/2005	705	1.36	-0.115	0.92	2708
mean				0.89	2558

Table 3 Calibrated values of Parameters

Parameter	Unit	Value
A_0	m^2	37822
a	km	16.7
D	m^2/s	2562
E_0	km	26.7
e	km	30
c	m/s	12
φ_0	rad/s	-0.7

Table 4 Calibration results of Song's model

	Dahu	Sishengwei	Zhangpeng	Dasheng
u_f(m/s)	-0.0175	-0.0317	-0.0527	-0.0937
υ (m/s)	1.8794	1.3512	1.0178	0.7390
D_S (m^2/s)	2269	2269	2269	2269

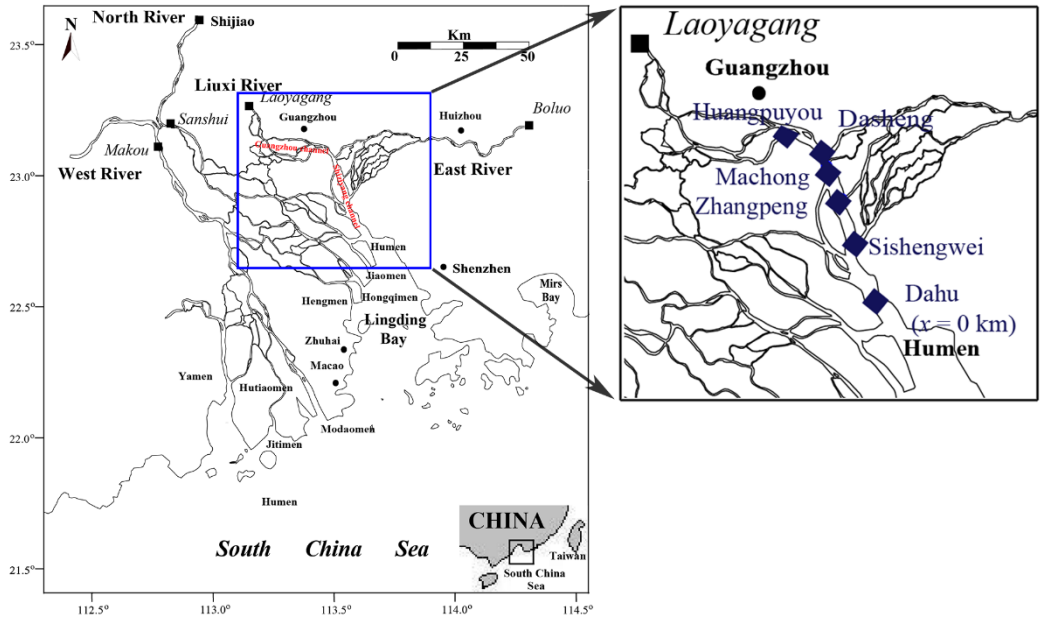

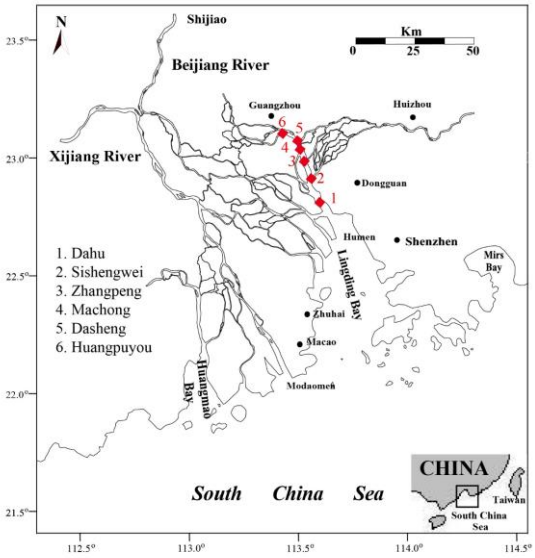

Figure 1: Map of the Humen estuary, showing the gauging stations where salinity concentration was measured ~~where salinity measurements were taken~~ during the~~a~~ field survey from 29 ~~Jan.~~January ~~29th~~ to 3 ~~Feb.~~February ~~3rd~~, 2005.

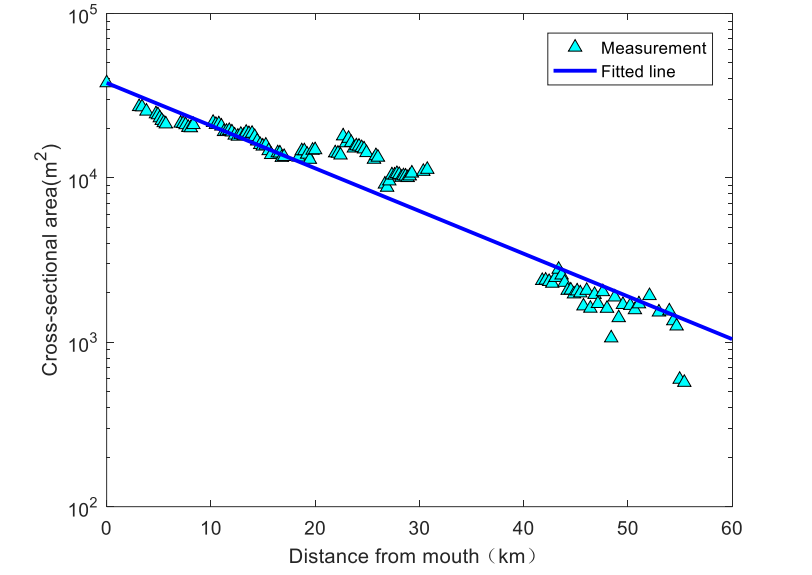

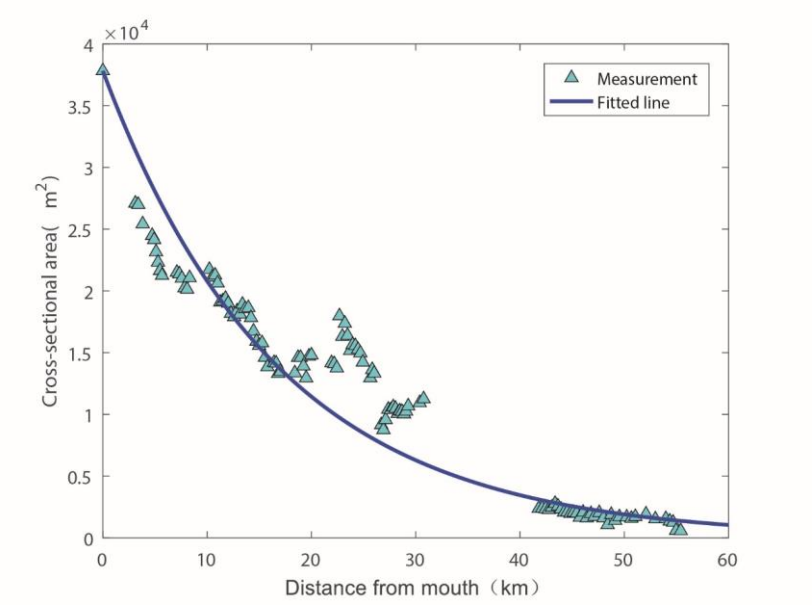

Figure 2: Shape of the Humen estuary ~~waterway~~, showing the correlation between the cross-sectional area A (m^2) and the distance from the estuary mouth x (km). The coefficient of determination R^2 is =0.92. The triangles represent observations and the line represents the fit to ~~Triangles represent observations and the fitted line represents the exponential in~~ Eq. (1), where the area at the estuary mouth A_0=37822 m^2 and the area convergence length (a) is 16.7 km.

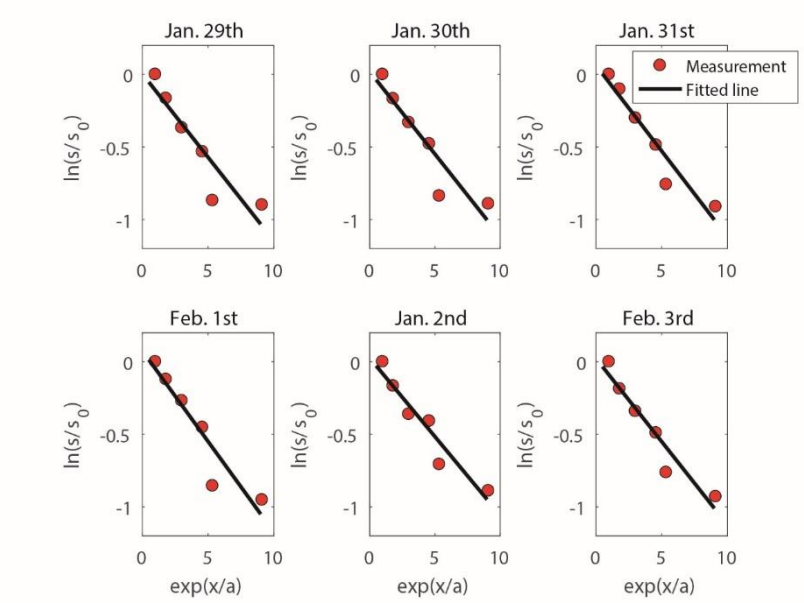

Figure 3: Relative salinity concentration along the Humen estuary~~Plots of $\ln(s/s_0)$ against $\exp(x/a)$ in the Humen estuary~~. The circlers represent observations and the lines represent the fit to~~Circles represent observation and the fitted lines represent~~ Eq. (12). ~~The linear relationship between these quantities predicted by Eq. (12) has been confirmed for all surveys, and the figures here show the linear line fitting results from Jan. 29th to Feb. 3rd.~~ ***s*** **is the salinity at distance** ***x*** **from the estuary mouth,** s_0 **is the salinity at the mouth and** ***a*** **is the convergence length of the cross-section area.**

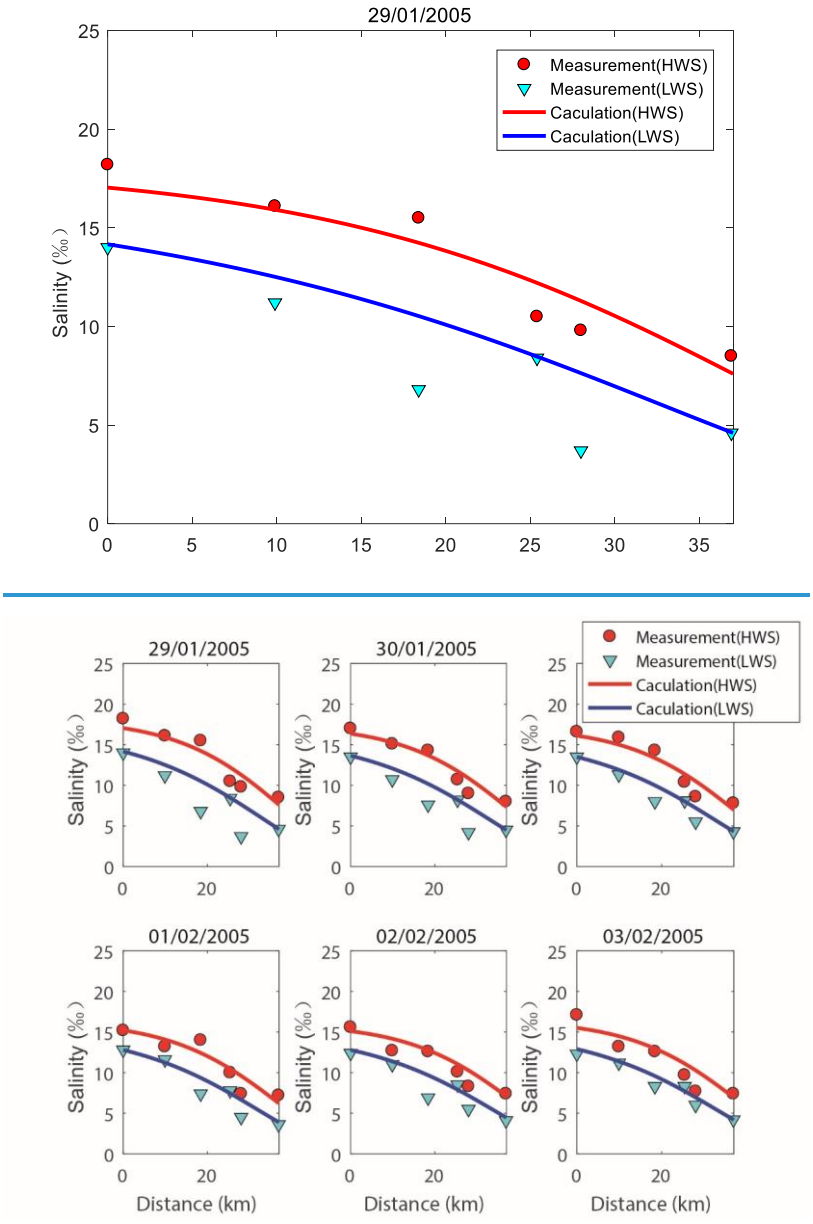

Figure 4: Comparison between calibration results and measured salinity concentration along the river on 29 January, 2005, showing values of measured salinity at high water slack (circles) and low water slack (inverted triangles), and the calibrated salinity curves at high water slack (red curve) and low water slack (blue curve).

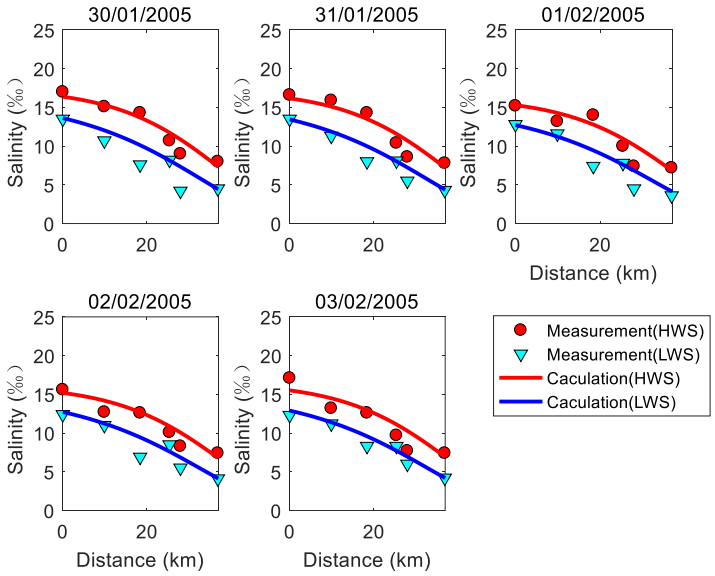

Figure 5: Comparison between validation result and measured salinity concentration along the river from 30 January to 3 February, 2005. ~~Calculated salinity distribution compared to measurements from Jan. 29th to Feb. 3rd, 2005, showing values of measured salinity at high water slack (circle) and low water slack (inverted triangle), and the calibrated salinity curves at high water slack (red curve) and low water slack (blue curve).~~

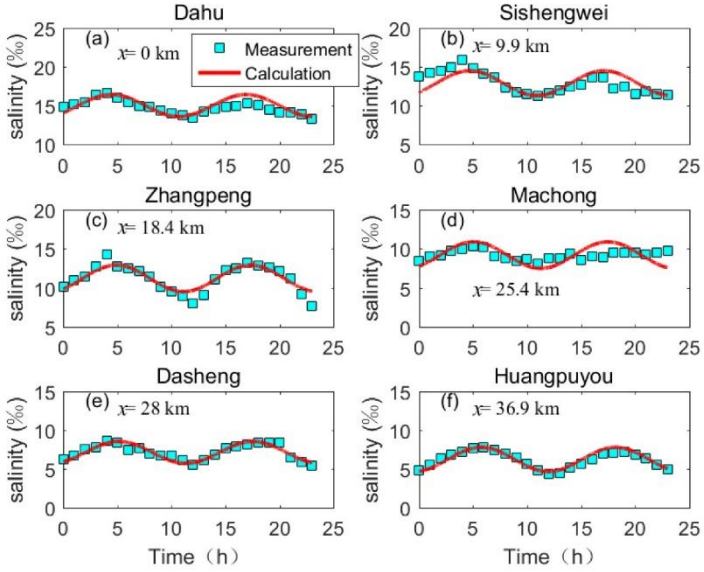

Figure ~~65~~: Comparison between the predicted and measured salinity concentration over time ~~Comparison of the simulated values with the measured values~~ on 31 ~~Jan.~~January ~~31~~ (neap tide) at each study site, showing that the analytical model captures the temporal variation of salinity. The hourly salinity measurements are represented by Rectangles ~~inverted triangles~~, while the simulated salinity varying with time is represented by the red solid line. In the figure, *x* is the distance from the estuary mouth.

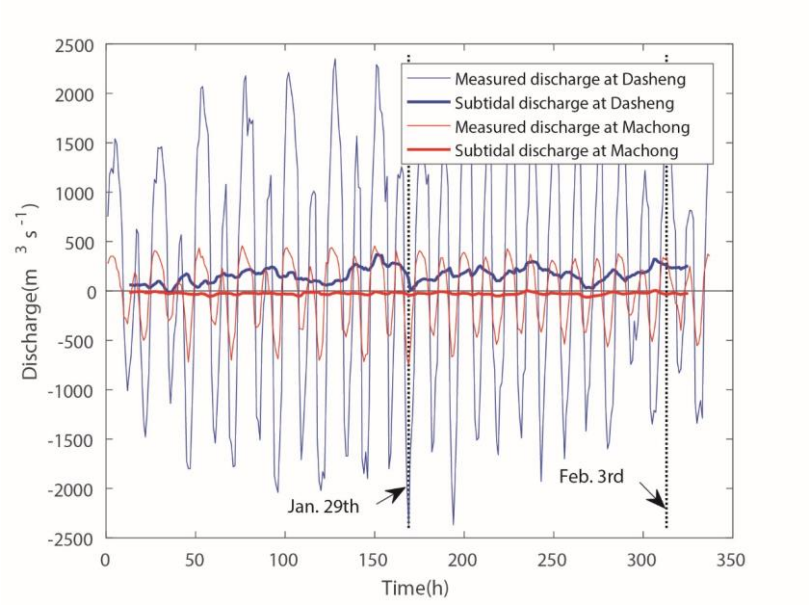

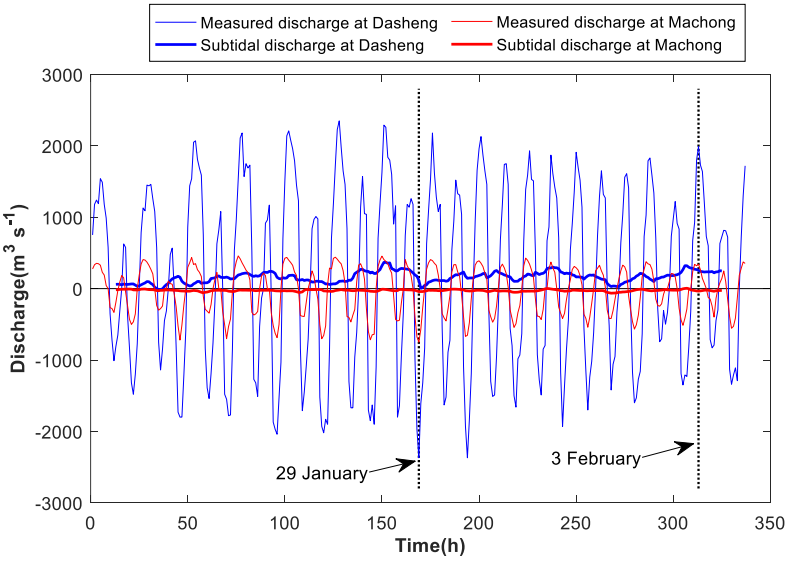

Figure 76: Subtidal discharge measured at Machong station and Dasheng station from 29 ~~Jan.~~January ~~29th~~ through 3 ~~Feb.~~February ~~3rd~~. Positive values mean~~s~~ seaward. ~~The subtidal discharge switches from seaward to landward between Machong and Dasheng stations, which will have an impact on salinity dynamics.~~

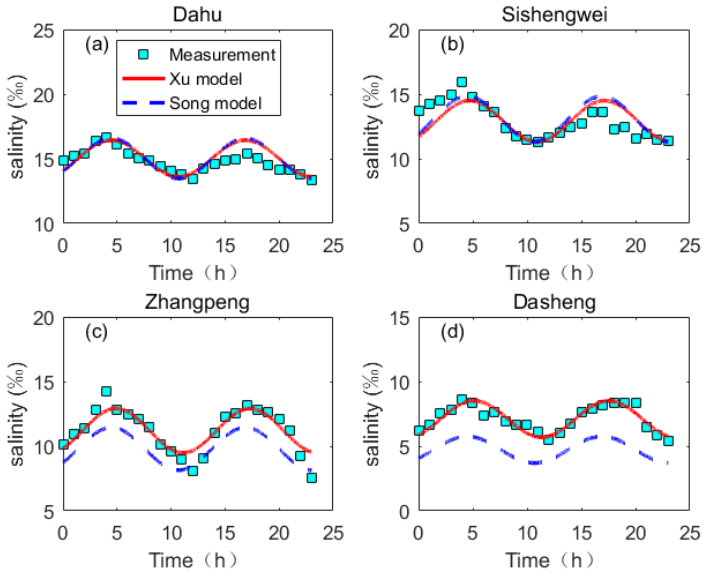

Figure 8: Comparison between observed and computed salinity concentration over time on 31 January (neap tide) at study sites along the Humen estuary.

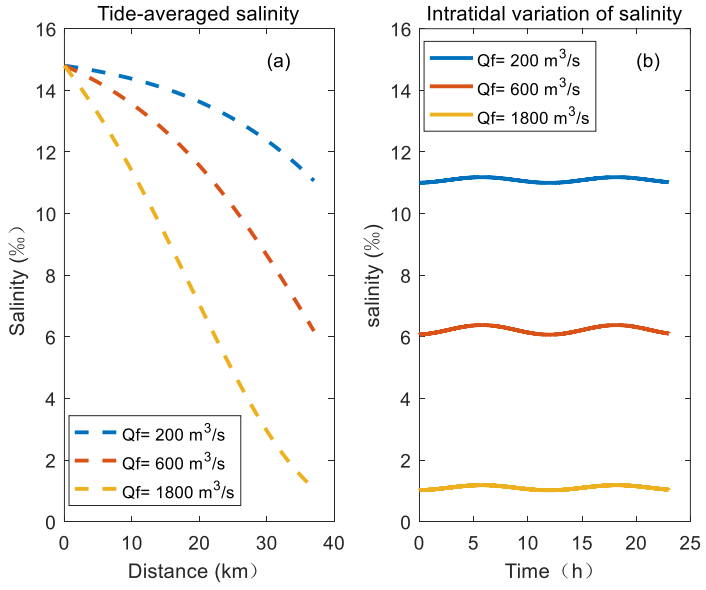

Figure 9: (a) longitudinal salt intrusion curve at Tidal average considering different river discharge; (b) intratidal variation of salinity at Huangpuyou station on 31 January, 2005 considering different river discharge.

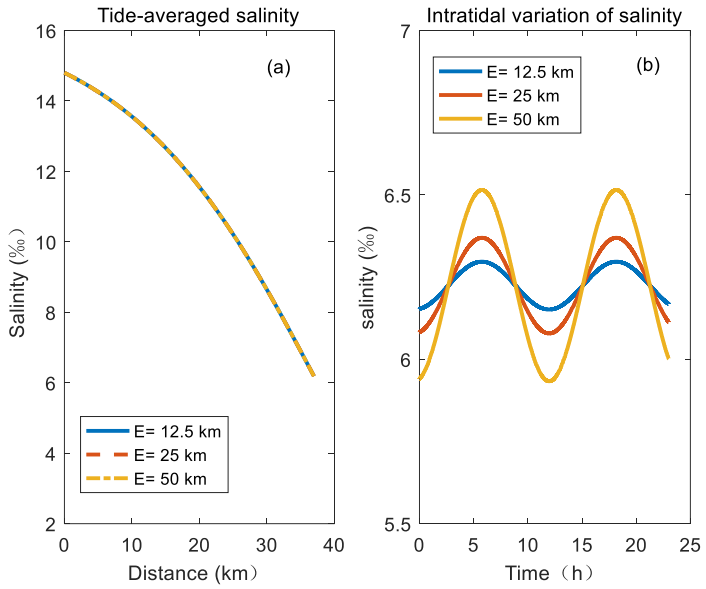

Figure 10: (a) longitudinal salt intrusion curve at Tidal average considering different tidal excursion; (b) intratidal variation of salinity at Huangpuyou station on 31 January, 2005 considering different tidal excursion.

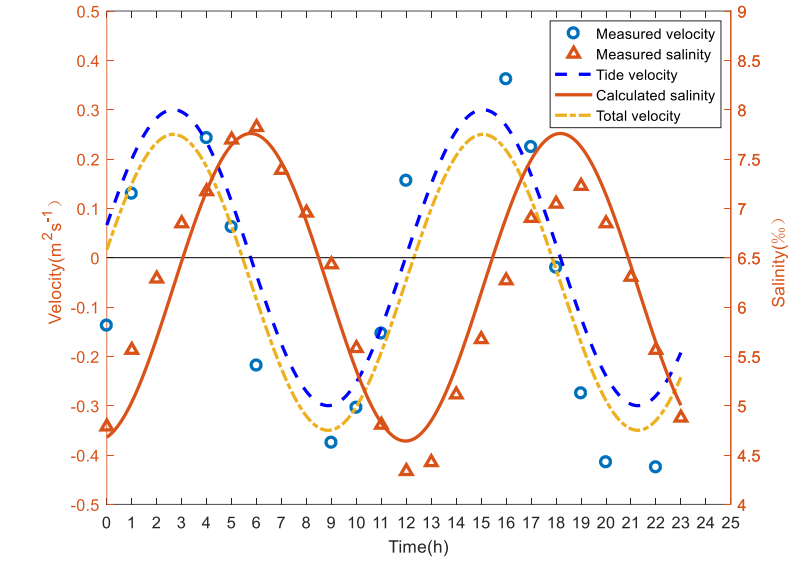

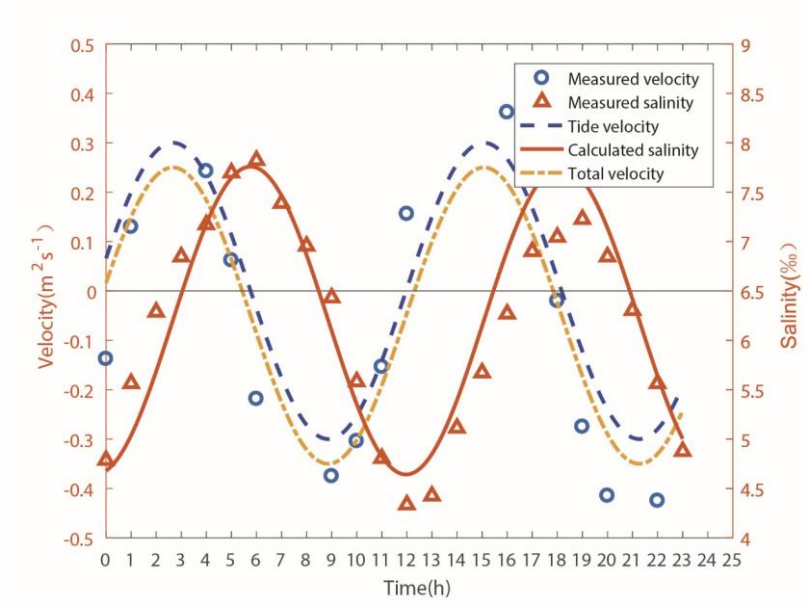

Figure ~~7~~11: Salinity and tidal flow velocity over a tidal cycle at Huangpuyou station. The measured salinity is represented by triangles and the measured flow velocity is indicated by circles (on 31 ~~Jan.~~January ~~31st,~~ 2005). The dashes line is the calculated tidal velocity while the dash-dotted line is the total velocity of tidale flow and river flow. The red solid curve represents salinity simulated by the unsteady analytical solution, which reproduces the time lag HWS and maximum salinity.

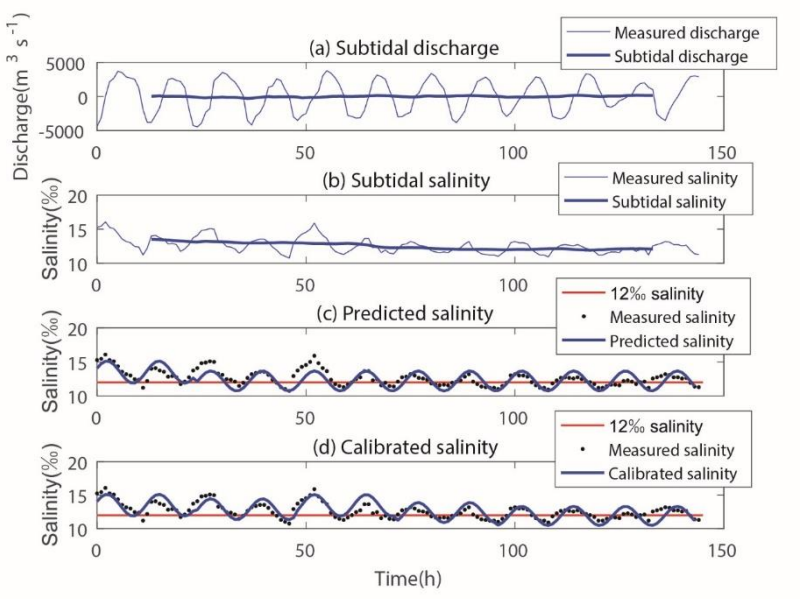

Figure ~~8~~12: Time for water intake of given salinity that is higher than 12‰. (a) Slight changes of the subtidal discharge; (b) Decreasing trend of subtidal salinity; (c) Predicted salinity in basis of observed data on 29 ~~Jan.~~January ~~29th~~; (d) Calibrated salinity in basis of observed data from 29 ~~Jan.~~January ~~29th~~ to 3 ~~Feb.~~February ~~3rd,~~ 2005.